2-Anilino-4-(thiazol-5-yl)pyrimidine CDK Inhibitors: Synthesis, SAR Analysis, X-ray Crystallography, and Biological Activity

Shudong Wang,[‡] Christopher Meades,[‡] Gavin Wood,[‡] Andrew Osnowski,[‡] Sian Anderson,[‡] Rhoda Yuill,[‡] Mark Thomas,[‡] Mokdad Mezna,[‡] Wayne Jackson,[‡] Carol Midgley,[‡] Gary Griffiths,[‡] Ian Fleming,[‡] Simon Green,[‡] Iain McNae,[†] Su-Ying Wu,[†] Campbell McInnes,[‡] Daniella Zheleva,[‡] Malcolm D. Walkinshaw,[†] and Peter M. Fischer*,[‡]

Cyclacel Limited, James Lindsay Place, Dundee DD1 5JJ and Structural Biochemistry, The University of Edinburgh, Michael Swann Building, King's Buildings, Edinburgh, EH9 3JR, Scotland, UK

Received August 7, 2003

Following the identification through virtual screening of 4-(2,4-dimethyl-thiazol-5-yl)pyrimidin-2-ylamines as moderately potent inhibitors of cyclin-dependent kinase-2 (CDK2), a CDK inhibitor analogue program was initiated. The first aims were to optimize potency and to evaluate the cellular mode of action of lead candidate molecules. Here the synthetic chemistry, the structure-guided design approach, and the structure−activity relationships (SARs) that led to the discovery of 2-anilino-4-(thiazol-5-yl)pyrimidine ATP-antagonistic CDK2 inhibitors, many with very low nM K_is against CDK2, are reported. Furthermore, X-ray crystal structures of four representative analogues from our chemical series in complex with CDK2 are presented, and these structures are used to rationalize the observed biochemical SARs. Finally results are reported that show, using the most potent CDK2 inhibitor compound from the current series, that the observed antiproliferative and proapoptotic effects are consistent with cellular CDK2 and CDK9 inhibition.

Introduction

The fidelity of progression through the human cell cycle is interrogated at various checkpoints in order to ensure the integrity of daughter cells. If errors in DNA replication are detected, normal proliferating cells undergo programmed cell death (apoptosis). Transformed cells, however, gain a proliferative advantage by bypassing or overriding these checkpoints. CDKs are intimately associated with the regulation of cell cycle progression.[1] Cyclins, the activating subunits of CDKs, are expressed specifically during certain phases of the cycle. Thus D-type cyclins appear in G1 and associate with CDKs 4 and 6. Later cyclin E is expressed and forms an active complex with CDK2. The action of these complexes on various substrates, and the retinoblastoma tumor suppressor protein (pRb), in particular, permits passage into S phase by dissociating the complex between pRb and E2F transcription factors. Next in turn is cyclin A, which associates with CDK2 and maintains pRb hyperphosphorylation. Later in S phase, however, cyclin A/CDK2 fulfills another important function, i.e. phosphorylation and deactivation of E2F.[2] This activity is necessary for progression and inappropriate E2F transcriptional activity in late S phase constitutes an apoptotic trigger.[3] This suggests that inhibition of cyclin A/CDK2 during S phase would lead to S-phase arrest, inappropriately persistent E2F-1 activity, and apoptosis. Tumor cells with disrupted pRb regulation would have higher levels of active E2F, which may leave them more vulnerable to the effects of persistent E2F

activity than normal cells, and it has in fact been shown that tumor cells are selectively sensitive to inhibition of cyclin A/CDK2.[4] Finally, entry and progression through mitosis are controlled by cyclin B/CDK1 activities. Furthermore, there exist several additional cyclin/CDK complexes, many of them with activities related to the cell cycle, but also in the regulation of transcription. Thus CDKs 7, 8, and 9 have all been implicated in modulation of RNA elongation by phosphorylation of the C-terminal domain of RNA polymerase II.[5]

Many ATP-antagonistic CDK inhibitor molecules have been discovered (reviewed in refs 6−8), and some of them have now reached clinical evaluation.[9,10] It nevertheless remains somewhat unclear what selectivity profile a CDK inhibitor should have for optimal anticancer activity. For example, a dominant-negative form of CDK2 devoid of catalytic activity was shown to prevent growth of cells in culture.[11,12] On the other hand, certain osteosarcomas and pRb-negative cervical cancers were shown to continue to proliferate after depletion of CDK2,[13] and CDK2-knockout mice appear to develop normally.[14,15] Our work has been guided by the most selective clinical CDK inhibitor, i.e. CYC202 (*R*-roscovitine), whose main targets are CDK2 and CDK9,[16] as well as by the hypothesis that CDK2 inhibition may provide a way of interfering selectively with cancer cells.[17] We recently reported the identification of 2-anilino-4-(thiazol-5-yl)pyrimidines as CDK2 inhibitors using virtual screening methods.[18] Here we describe our results to date with compounds from this new pharmacophore.
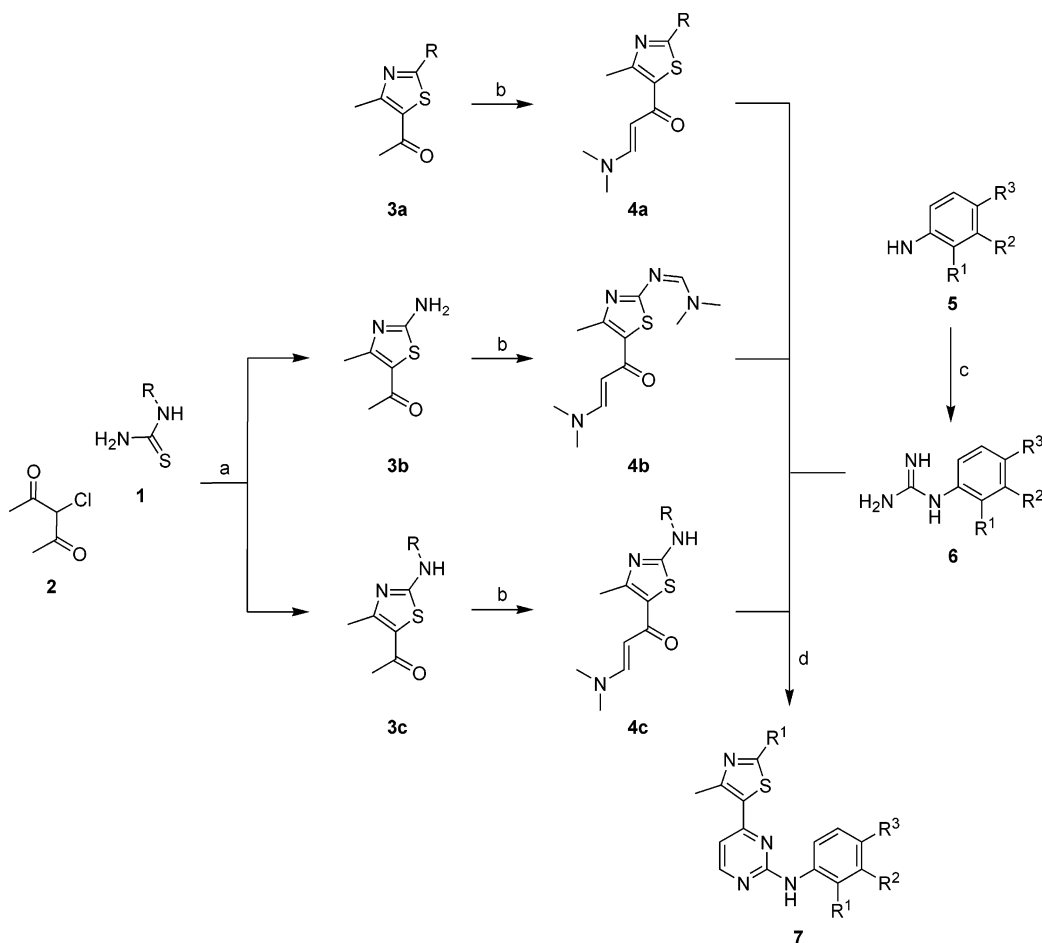
Chemistry

2-Amino-4-(thiazol-5-yl)pyrimidines (Scheme 1) were synthesized by the general pyrimidine condensation
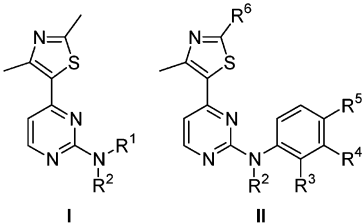
Scheme 1[a]

[a] Reagents: (a) pyridine, MeOH; (b) *N,N*-dimethylformamide dimethyl acetal, 120 °C; (c) HNO_3, aq cyanamide, 100 °C; (d) NaOH, 2-methoxyethanol, 125 °C.

method of Bredereck.[19] Unless commercially available, 5-acetyl-thiazoles **3** were prepared from the appropriate thioureas **1** and 3-chloro-2,4-pentadione **2** and were converted to the enaminones **4** by heating in *N,N*-dimethylformamide dimethyl acetal. Enaminones **4** were then condensed to the desired pyrimidines at elevated temperature in alcoholic alkali with guanidine carbonate. When it was found that introduction of anilino groups at the pyrimidine C2 position dramatically increased the biological activity of the resulting compounds in both enzymatic and cell-based assays, a number of 2-phenylamino-4-(thiazol-5-yl)pyrimidines **7** were designed and prepared. The anilino guanidines were derived from the corresponding anilines **5** by treatment of their nitrate or hydrochloride salts with cyanamide.[20] Synthesis of 4-*N,N*-dimethylamino-3-chlorophenyl guanidine was conducted by the sequence in Scheme 1, starting from 3-chloro-4-fluoronitrobenzene. Selective displacement of the fluorine was achieved by heating this compound with *N,N*-dimethylamine hydrochloride in DMSO in the presence of potassium carbonate in a sealed tube. The nitro group in the product was subsequently reduced with Fe/HOAc to the primary amine and further treated with cyanamide to afford the corresponding guanidine. Similarly, 3-nitro-4-*N,N*-dimethylamino anilino guanidine was prepared by nucleophilic displacement at C4 of 4-fluoro-3-nitroaniline. From the acetylthiazole **3b**, which contains a primary amino group, the enaminone was obtained in the imino

form **4b**. This compound could be used directly in the following pyrimidine ring formation reactions, during which the amino group (**7**, $R^1 = NH_2$) was regenerated.

Results and Discussion

Initial SAR and Design. We recently reported the discovery of a new 2-amino-4-heteroarylpyrimidine ATP-antagonist CDK inhibitor pharmacophore through virtual screening and structure-based design.[18] One of the lead compounds from the screening was the dimethylthiazoloaminopyrimidine **8** (Table 1), which possessed modest CDK2 inhibitory potency. Inspection of the binding mode of this compound in the ATP pocket of a CDK2 complex crystal structure[18] revealed that it bound in a similar way to ATP itself (Figure 1). In both cases a group of three H-bonds between the ligand and the backbone of CDK2 residues Glu81 and Leu83 was observed, interactions that are conserved in most kinase inhibitor complexes. In the ATP structure[21] the guanine amino group donates a H-bond to the carbonyl of Glu81, whereas N1 and H2 of the purine system accept and donate H-bonds to the amide NH and carbonyl of Leu83, respectively. Compound **8** formed similar H-bonding contacts through the NH_2 (Glu81 CO), pyrimidine N1 (Leu83 NH), and H6 (Leu83 CO). The dimethylthiazole ring overlaps roughly with the space occupied by the ribose system in ATP. As expected from this binding mode, we found that bismethylation of the primary

Table 1. Inhibition of CDK Activity and Tumor Cell Proliferation

compd	formula	R^1	R^2	R^3	R^4	R^5	R^6	K_i (μM)[a]		72-h MTT IC$_{50}$ (μM)[b]
								CDK2	CDK4	
8	I	H	H	–	–	–	–	6.5 ± 3.0	16 ± 9	>10
9	I	Me	H	–	–	–	–	>20	>20	>10
10	I	Me	Me	–	–	–	–	>20	>20	>10
11	II	–	H	H	H	H	Me	0.08 ± 0.02	2.6 ± 0.2	4.9 ± 1.1
12	II	–	H	Cl	H	H	Me	>20	>20	>10
13	II	–	H	H	Cl	H	Me	0.67 ± 0.10	9.4 ± 0.1	1.7 ± 2.2
14	II	–	H	H	H	Cl	Me	2.5 ± 1.5	>20	>10
15	II	–	H	F	H	H	Me	1.2 ± 0.4	1.2 ± 0.7	>10
16	II	–	H	H	F	H	Me	0.10 ± 0.05	0.9	2.0 ± 0.9
17	II	–	H	H	H	F	Me	0.04 ± 0.03	>20	6.8 ± 1.9
18	II	–	H	CF$_3$	H	H	Me	>20	>20	>10
19	II	–	H	H	CF$_3$	H	Me	>20	>20	>10
20	II	–	H	H	H	CF$_3$	Me	0.29 ± 0.24	>20	2.3 ± 1.7
21	II	–	H	H	OH	H	Me	0.06 ± 0.03	0.21 ± 0.16	1.2 ± 0.6
22	II	–	H	H	OH	H	NHMe	0.11 ± 0.10	0.37 ± 0.02	1.6 ± 1.1
23	II	–	H	H	OH	H	NHEt	>10	>20	>10
24	II	–	H	H	H	OH	Me	0.14 ± 0.12	0.32 ± 0.18	2.0 ± 2.6
25	II	–	H	H	H	OH	NHMe	0.07 ± 0.06	0.32 ± 0.27	1.0 ± 0.2
26	II	–	H	H	H	OH	NH$_2$	0.030 ± 0.005	0.32 ± 0.21	0.2 ± 0.2
27	II	–	H	H	NO$_2$	H	Me	0.11 ± 0.03	>20	1.0 ± 0.7
28	II	–	Me	H	NO$_2$	H	Me	>20	>20	>10
29	II	–	H	H	NO$_2$	H	NMe$_2$	0.06 ± 0.02	5.3 ± 2.9	2.8 ± 0.5
30	II	–	H	H	NO$_2$	H	NHMe	0.80 ± 0.55	1.6 ± 0.1	3.4 ± 0.8
31	II	–	H	H	NO$_2$	H	NHAll	0.16 ± 0.07	7.1 ± 4.1	0.5 ± 0.0
32	II	–	H	H	NO$_2$	H	NH$_2$	0.0020 ± 0.0006	0.053 ± 0.005	0.3 ± 0.1
33	II	–	H	H	NO$_2$	H	pyrid-2-yl	>20	>20	>10
34	II	–	H	H	H	NO$_2$	Me	4.1 ± 1.4	>20	>10
35	II	–	H	H	NH$_2$	H	Me	0.40 ± 0.02	10.64 ± 0.05	2.1 ± 1.4
36	II	–	H	H	CN	H	Me	0.30 ± 0.45	0.48 ± 0.11	1.5 ± 0.9
37	II	–	H	H	H	NMe$_2$	Me	0.22 ± 0.21	0.96 ± 0.69	0.6 ± 0.5
38	II	–	H	H	NO$_2$	NMe$_2$	Me	0.020 ± 0.025	0.27 ± 0.13	0.6 ± 0.4
39	II	–	H	H	Cl	NMe$_2$	Me	0.10 ± 0.08	1.0 ± 0.5	0.2 ± 0.2
40	II	–	H	H	H	NMe$_2$	NH$_2$	0.70 ± 0.25	0.90 ± 0.26	2.3 ± 0.2

[a] Average values from at least 4 independent determinations (± 1 standard deviation). [b] anti-proliferative activities (72-h MTT IC$_{50}$ values ± 1 standard deviation) quoted are the averages from measurements using the human tumor cell lines A549, HT29, and SaOS-2 (3 independent determinations each).
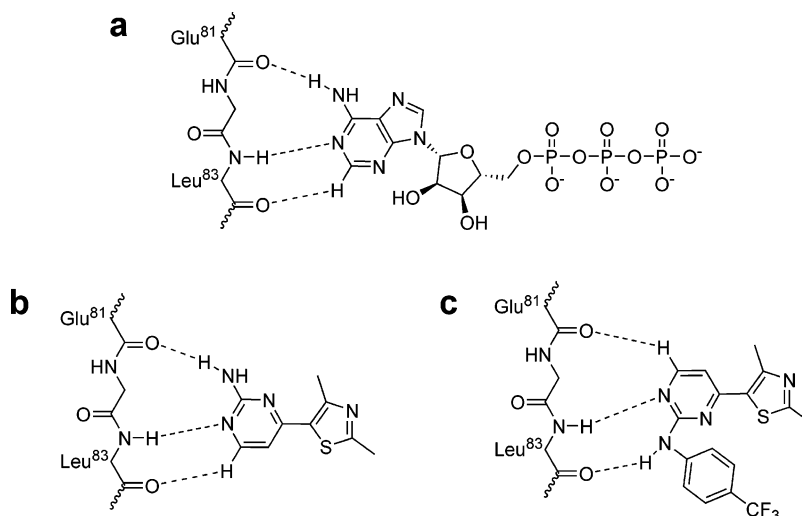
Figure 1. H-Bonding interactions of ATP (a) and compounds **8** (b), and **20** (c) with the backbone of CDK2 residues Glu81 and Leu83.

amino group on the pyrimidine ring had a detrimental effect on binding and in fact abolished biological activity

completely (**10**). Surprisingly, however, monomethylation (**9**) had the same effect, despite the fact that one

would expect that the methylamino function should still be able to form a similar H-bond with the CDK2 Glu81 carbonyl group as the primary amino group of compound **8**. In any case, introducing an aromatic substituent to this amino function is not only tolerated, but actually results in a significant potency increase. Thus the aniline derivative **11** is almost 100-fold more potent in inhibition of substrate phosphorylation by CDK2 than the corresponding amine **8**. Furthermore, during the SAR studies addressing the anilino part of the pharmacophore, we succeeded in obtaining a CDK2 complex crystal structure of a relevant compound (**20**). Prior to this a pharmacophore hypothesis was proposed for the aniline derivatives based on molecular dynamics docking techniques and was used in the initial design phases. The structural solution confirmed this hypothesis and showed a different binding mode with respect to the pyrimidine ring compared to compound **8**.[18] In this alternative pose the H-bonds referred to above now were as follows: pyrimidine H6 (Glu81 CO), N1 (Leu83 NH), and anilino NH (Leu83 CO); i.e., the pyrimidine ring in the CDK complex of **20** was in the same plane but flipped through 180° compared to **8** (Figure 1). As a result, the phenyl group of **20** pointed out toward the entrance of the binding cleft in an area that is not occupied by ATP.

Optimization of the In Vitro Potency. Examination of the initial docked ligands and the subsequent crystal structures provided insight for the design of more potent analogues. To pick up potential additional interactions with any of the numerous polar residues lining the rim of the ATP binding cleft, we envisaged substitution of the phenyl ring and modification of the thiazol-2-yl methyl group in, for example, compound **11**. We first investigated the effect of substituents on the aniline moiety while leaving the dimethylthiazole ring unchanged. In general we found that only electron-withdrawing substituents preserved or enhanced CDK2 inhibitory potency. Furthermore, this effect was only observed when such groups were introduced in the meta- or para-position of the aniline, whereas the corresponding ortho-substituted analogues were generally less active or inactive. For example, of the chloro-anilines **12**−**14** the meta-isomer **13** was somewhat less potent than the unsubstituted aniline **11**, whereas the para-isomer **14** was less potent and the ortho-isomer possessed only marginal activity. A similar situation was seen with the more potent fluoroanilines **15**−**17**; except here the para-isomer **17** was most potent. Of the corresponding trifluoromethyl compounds **18**−**20**, only the para-isomer **20** displayed significant biological activity. When a hydroxyl group was introduced, this was found to maintain potency with respect to the unsubstituted analogue **11**, both in the para- (**24**) and particularly in the meta-isomer **21**. Furthermore, cellular antiproliferative potency was now also enhanced. The *m*-nitro compound **27** was somewhat less effective than the reference compound **11** as a CDK2 inhibitor, but displayed about 5-fold higher cellular activity. The corresponding *p*-nitro isomer **34**, on the other hand, was practically devoid of activity. To reconfirm the importance of the anilino NH function as a H-bond donor, we prepared and tested an *N*-methyl derivative of compound **27**; as expected, this analogue **28** was inactive.

Finally amino (**35**) and nitrile (**36**) substituents in the anilino meta-position also furnished potent compounds.

We next turned our attention to modification of the thiazole system. Whereas the thiazol-4-yl methyl group makes near-optimal hydrophobic contacts with Phe80 of CDK2 (Figure 2), the thiazol-2-yl methyl group is positioned in the vicinity of several polar residues, particularly Asn132. We therefore expected that introduction of groups capable of H-bonding should be favorable. We investigated this in the context of the optimal *m*-/*p*-hydroxy- and *m*-nitroanilino pyrimidin-2-yl systems. However, replacement of the thiazol-2-yl methyl group with a methylamino group (compounds **22**, **25**, and **30**) did not change potency appreciably. Placement of bulkier secondary amino groups, e.g. ethylamino (**23**) or pyrid-2-yl-amino (**33**), was not tolerated, with the exception of the allylamino group in the context of the *m*-nitroanilino system (**31**). A primary amino group in place of the thiazol-2-yl methyl group preserved activity (**26**); again the *m*-nitroanilino system provided a different context, and here the primary amino derivative **32** was a particularly potent CDK2 inhibitor, although this potency gain was not accompanied in equal measure by increased cellular activity. The fact that a dimethylamino (**29**) replacement preserved activity indicated that a H-bond acceptor group was favorable in place of the thiazol-2-yl methyl group.

As discussed above, a comparatively poor correlation between the biochemical and cellular potency of the various test compounds was observed. Nevertheless, the fact that compounds with poor potency or no activity against isolated CDK enzymes were also devoid of cytotoxic activity strongly suggests that the antiproliferative effects are a consequence of cellular CDK inhibition. It cannot be ruled out, however, that inhibition of other cellular (protein kinase) targets contributes to the antiproliferative activities observed. Unlike biochemical activity, cellular potency is affected by such factors as membrane permeability, protein binding, solubility, and stability in physiological medium. These factors, as well as metabolism, also affect in vivo absorption and disposition and are therefore of prime importance in terms of bioavailability. Overall the compounds discussed thus far were found to be comparatively lipophilic and poorly water-soluble. This situation was improved with compounds that contained a *p*-dimethylamino substituent in the anilino portion (**37**−**40**). Combination of this group in **37** with otherwise favorable meta-anilino substituents such as chloro (**39**), and nitro (**38**), led to soluble nM CDK2 inhibitor compounds with good cellular activity. Combination with the thiazol-2-yl primary amino group (**40**) discussed above, on the other hand, did not improve potency. As previously, antiproliferative potency did not follow biochemical CDK2 inhibition potency gains in the *p*-(dimethylamino)aniline series **37**−**40**, either. We are currently evaluating compounds from this series for their in vivo antitumor effects. Furthermore, we have chosen our most potent CDK2 inhibitor, i.e., compound **32**, to verify that the antiproliferative effects observed correlate with cellular CDK inhibition (see below).

X-ray Crystallography. Structural data for the four new inhibitor/CDK2 complexes are summarized in Table 2 and Figure 2. In each case, structure refinement gave
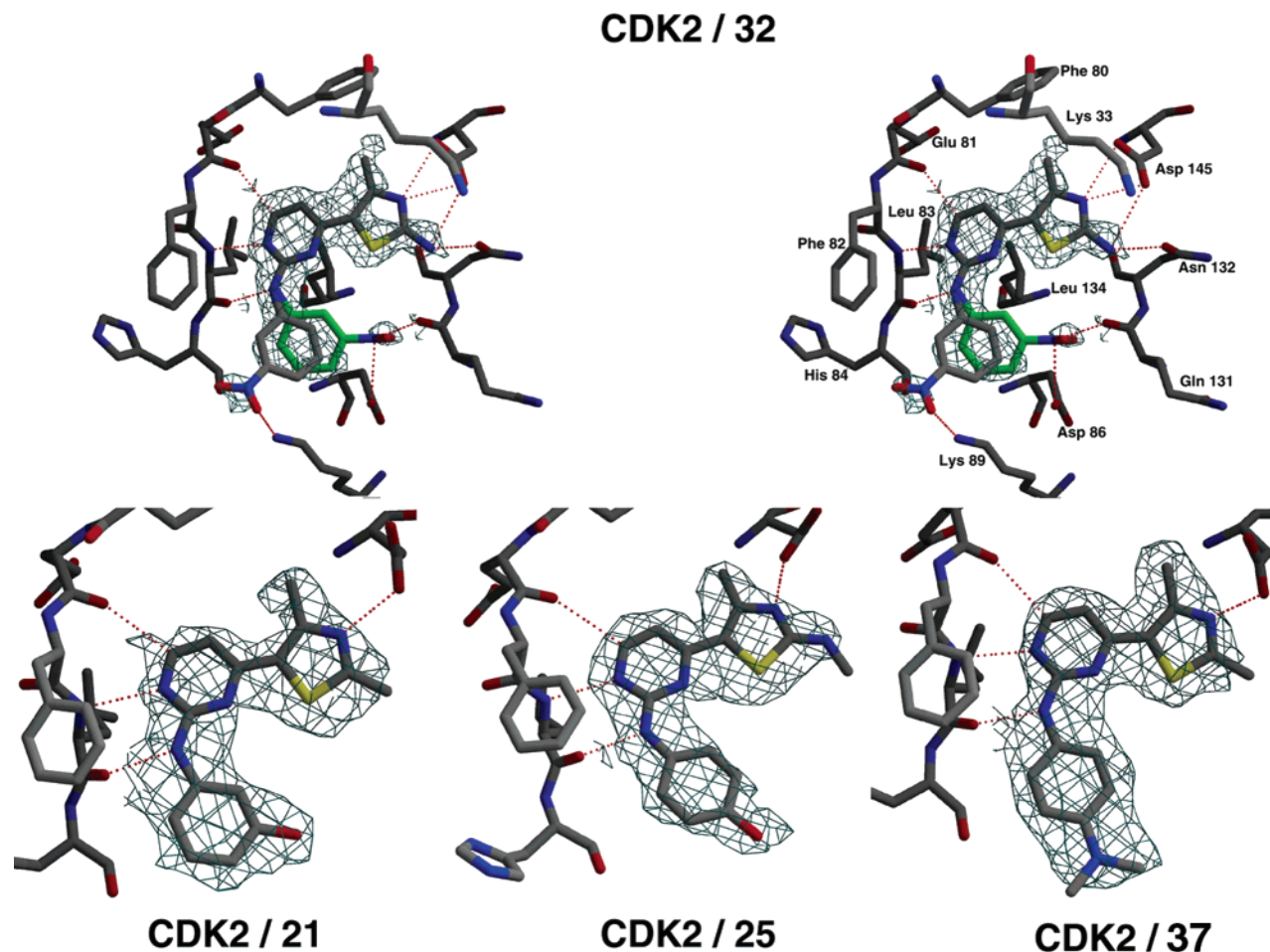
Figure 2. Inhibitor/CDK2 complex crystal structures. Electron density for all four ligands in the CDK2 crystal complexes solved. A stereoimage of the CDK2/**32** is shown at the top. The H-bonds are indicated with red broken lines. The two positions of the nitro group are distinguished from each other by one of the rings being colored green. Asn132 is shown in the position that interacts with the NH_2 group.

Table 2. X-ray Data Collection and Structure Refinement

	CDK2/**21**	CDK2/**25**	CDK2/**32**	CDK2/**37**
resolution (Å)	25−2.53	25−2.5	15−1.96	23−2.3
(outer shell)	(2.69−2.53)	(2.66−2.5)	(2.07−1.96)	(2.44−2.3)
Unit cell	$a = 53.489$	$a = 52.896$	$a = 53.491$	$a = 53.337$
$P2_12_12_1$	$b = 71.987$	$b = 70.002$	$b = 72.232$	$b = 71.794$
($\alpha = \beta = \gamma = 90°$)	$c = 72.362$	$c = 71.709$	$c = 72.578$	$c = 71.414$
total reflections observed	91355	102882	226048	78546
unique reflections	9820	9345	20604	12686
multiplicity	9.30	11.0	10.97	3.4
R_{merge} % (outer shell)	11.7 (50.7)	8.9 (49.0)	5.9 (16.5)	5.0 (14.8)
$\langle I/\sigma(I) \rangle$ (outer shell)	12.8 (3.38)	13.8 (2.76)	22.4 (7.7)	3.8 (4.9)
completeness % (outer shell)	99.9 (100)	96.4 (96.7)	99.4 (99.9)	98.7 (96.7)
R_{work} %	22.1	23.0	21.8	23.0
R_{free} %	28.0	27.7	23.7	27.3
RMS bonds (Å);	0.007/	0.010/	0.006/	0.006/
RMS angles (deg)	1.3	1.5	1.3	1.2
refined ligand occupancy %	97	98	80	80

rise to electron density maps that permitted unambiguous placement of the ligand structure in the active site of CDK2. The binding poses in the ATP pocket are similar for the four ligands. In each case, the characteristic H-bonding network involving the Glu81 and Leu83 backbone is observed. Furthermore, the Leu134 side chain forms strong hydrophobic interactions with the pyrimidine and anilino rings and the thiazol-4-yl methyl groups always pack up against the Phe80 phenyl ring. The Asp145 carboxyl group forms a polar interaction with the ligand thiazole N atom in each complex;

in the case of **21**, **25**, and **37**, this carboxyl also interacts directly with the Lys33 side chain amino function. In all four CDK-ligand structures the conformation of the side chain of Lys33 adopts a different conformation to that found in the native CDK structure and the T-loop (residues 147−165) is disordered. This observation fits with the suggested mechanism for ligand-induced disordering of the activation loop.[18]

The K_i values for the four compounds in this chemically related series generally correlate with the number of observed H-bonds, van der Waals interactions, and

Table 3. Selectivity of Kinase Inhibition by Compound **32**

protein kinase	K_i (nM)[a]
CDK1/cyclin B	80 ± 40
CDK2/cyclin E	2.0 ± 0.6
CDK4/cyclin D1	53 ± 5
CDK7/cyclin H	70 ± 10
CDK9/cyclin T1	4 ± 3
ERK-2	>1000
PKCα	>1000
SAPK2A (p38)	>1000
CaMKII	>1000
Abl	160 ± 10
CKII	>1000
p70 S6	>1000
Akt/PKB	>1000
Plk1	>1000
PKA	>1000
GSK3β	20 ± 10

[a] Average values from at least four independent determinations (± one standard deviation).

polar interactions. The fact that both meta- and para-substituted anilino moieties are tolerated in the various thiazolopyrimidine inhibitors is consistent with the observed H-bonding interactions of the hydroxyl group with either the side chains of Asp86 (**21**) or Lys89 (**25**). Replacement of the thiazol-2-yl methyl group with NHMe (**25**) does not result in additional H-bonding interactions; however, for the most potent CDK2 inhibitor **32**, the presence of the primary NH_2 group leads to increased electrostatic interactions with the side chains of Asp145 and Asn132. The side chain of Asn132 is found to adopt two alternative conformations, only one of which interacts with the NH_2 group (Figure 2). The significantly tighter binding of **32** may also be explained by additional interactions involving the nitro substituent. Careful refinement showed that the nitrophenyl group was in fact disordered. In both orientations observed, the nitro group makes weak but favorable electrostatic interactions. Particularly notable is the interaction between the carboxyl group of Asp86 to the NO_2 nitrogen of 3.48 Å and a close contact with the backbone carbonyl of Gln131. In the alternative conformation there is a weak H-bond between the nitro group and the side chain of Lys89 (Figure 2). It has been observed from structures of CDK2/cyclin A that Asp145 undergoes a significant rearrangement upon cyclin binding.[22] The inhibitor complex structures presented here are with monomeric CDK2, and therefore the possibility cannot be excluded that the thiazole NH_2 in compound **32** makes more favorable contacts in the activated kinase. Overlay of the CDK2 complex of **32** with the CDK2/cyclin A complex (PDB accession code 1JST) suggests that this may indeed is the case, as Asp145 is significantly closer to the amino group. This observation could also explain the markedly lower potency of **32** against CDK1/cyclin B1 (Table 3). As the ATP clefts of CDK2 and CDK1 are highly conserved, large differences in inhibition would not be expected. It is conceivable, however, that activation of CDK1 by cyclin B leads to a different conformation of Asp146 (residue corresponding to Asp145 in CDK2), and perhaps of the ATP binding site in general, and hence could result in less favorable contacts in this context.

Biochemistry and Biology. The kinase selectivity of prototype compound **32** was investigated (Table 3). We found that potency was highest against CDK2, but
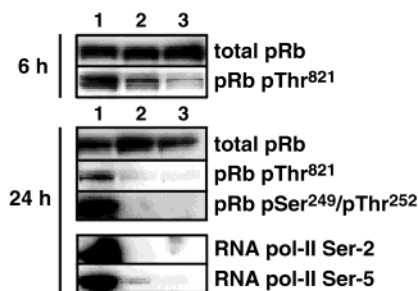

Figure 3. Western blot analysis of A549 cells 6 and 24 h posttreatment with (1) DMSO control; (2) 0.5 μM compound **32** (72-h MTT IC$_{50}$); (3) 2 μM compound **32**. Reduced phosphorylation of pRb at Thr821 and Ser249/Thr252 is observed, indicating cellular inhibition of CDK2 and CDK4, respectively. Phosphorylation is also reduced at the RNA polymerase II Ser-2 and Ser-5 sites, a possible indication of inhibition of CDK7 and CDK9. (The 6-h analysis was only performed for the pRB Thr821 phosphorylation).

other CDKs, particularly CDK9, were also inhibited at somewhat reduced potency. Unlike other small-molecule ATP-antagonist CDK inhibitors,[23] compound **32** did not have a significant effect on the catalytic activity of the structurally related ERK-2 MAP kinase. GSK3, on the other hand, which is also closely related to CDKs, was inhibited by **32** with sub-micromolar potency. Of the other protein kinases assayed, only the Ableson protein tyrosine kinase was inhibited appreciably.

The retinoblastoma tumor suppressor proteins (pRb, p107, p130) are the main physiological substrates for the G1/S CDK complexes (CDK4/cyclin D1, CDK2/cyclin E, and CDK2/cyclin A). The entry of cells into S phase requires CDK-mediated phosphorylation of pRb, releasing and activating transcription factors of the E2F family, which are held in inactive pRb/E2F complexes during the G0 and M phases.[1] We therefore sought to demonstrate inhibition of CDK2 activity in live cells by examining the effects on the phosphorylation state of pRb upon exposure of the cells to compound **32**. We found that when A549 (a lung adenocarcinoma cell line) cells were treated with compound **32**, a time- and dose-dependent decrease in phosphorylation of pRb at Thr821, a CDK2-preferential phosphorylation site of pRb,[24] was observed (Figure 3). Treatment with compound **32** also resulted in decreased phosphorylation at the Ser249/Thr252 residues of pRb, sites preferential for cyclin D/CDK4 phosphorylation,[24] and at the Ser-2 and Ser-5 sites of RNA polymerase II, sites potentially phosphorylated by CDKs 1, 7, 8, and 9.[25] Such a reduction in pRb phosphorylation demonstrates an inhibitory effect of compound **32** on cellular CDK2 and CDK4 activities, while the reduced phosphorylation at Ser-2 and Ser-5 of RNA polymerase II suggests potential inhibition of CDKs 9, 8, or 7. Such cellular inhibitions are in agreement with the in vitro kinase K_i values presented in Table 3 and would indicate a mode of action of compound **32** involving multiple CDKs.

To examine the effects of compound **32** on the cell cycle, A549 cells were synchronized at the G1/S boundary by sequential block and release using thymidine and mimosine.[26] Compound **32** was added at 0.5 μM concentration on the final release and subsequent progress through the cell cycle was monitored by fixing cells at several time points and analyzing DNA and cyclin B
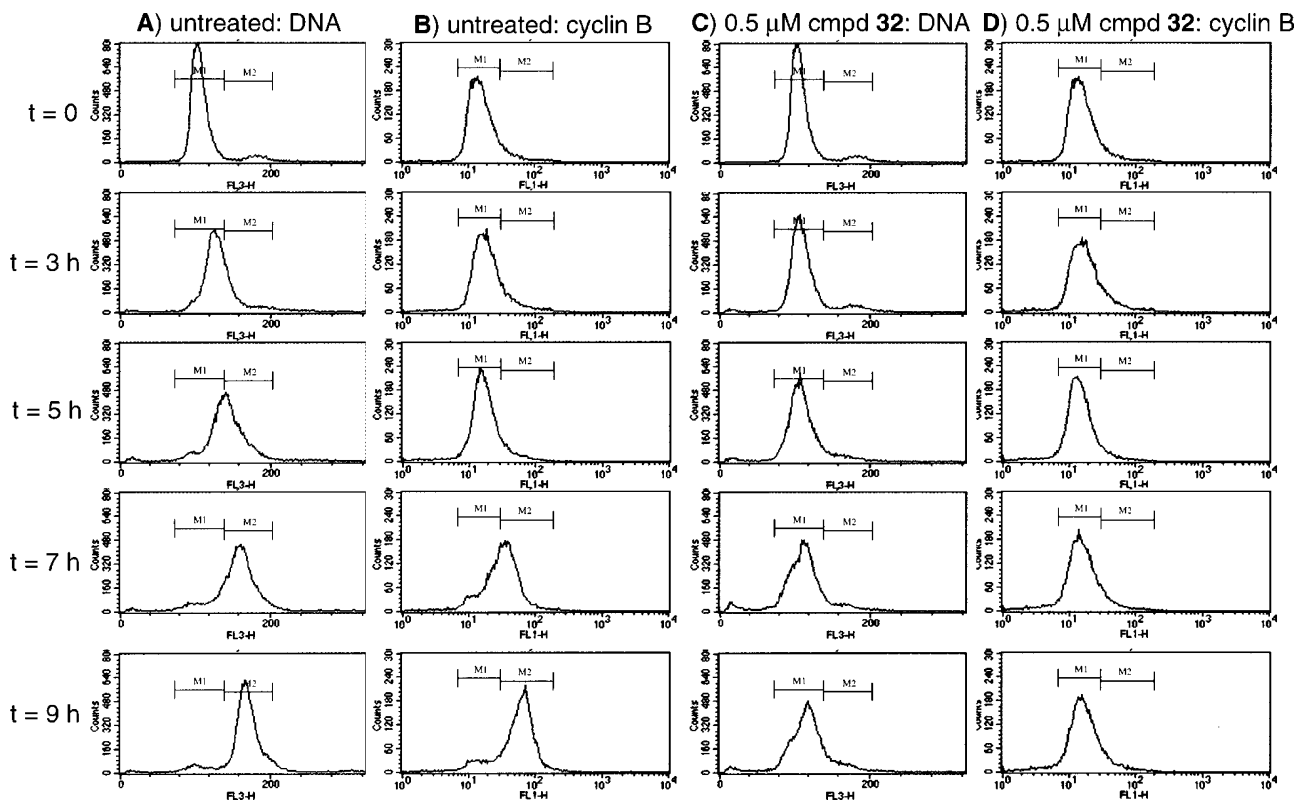
Figure 4. Compound **32** blocks cells in G1/S and prevents induction of cyclin B and entry into G2/M. Human A549 cells were synchronized using a sequential thymidine/mimosine block. Upon release of the block, cells were treated with compound **32,** and their synchronous passage through the cell cycle was followed up to 9 h by FACS analysis. Panel A: untreated cells labeled with propidium iodide to detect DNA content; panel B: untreated cells labeled with FITC-conjugated anti-cyclin B antibody; panel C: cells treated with 0.5 μM compound **32** at $t = 0$; labeled with propidium iodide to detect DNA content; panel D: cells treated with 0.5 μM compound **32** at $t = 0$, labeled with FITC-conjugated anti-cyclin B antibody.

content. On release the majority of untreated cells had a 2n DNA content and a low level of cyclin B ($t = 0$ in Figure 4) indicating synchronization at G1/early S. Over the following 6−7 h, the DNA content gradually increased, shown in panel A of Figure 4 as an increase in FL3 fluorescence, so that at 9 h the majority of cells had a 4n DNA content and high cyclin B levels (panel B in Figure 4), indicating that the cells had reached G2/M. However, the cells treated with compound **32** did not show the same increase in DNA content (panel C in Figure 4), and there was no increase in cyclin B levels (panel D in Figure 4), indicating that they were arrested in G1/early S and unable to exit S phase.

The effects of compound **32** on S-phase transition are consistent with the inhibition of CDK2. The generally accepted view is that cyclin D-dependent kinases initiate pRb phosphorylation in G1, and that cyclin E/CDK2 then completes the process, allowing activation of E2F-dependent transcription and coordinated expression of a number of genes required for DNA synthesis and subsequent S-phase progression. In addition, cyclin E/CDK2 and cyclin A/CDK2 phosphorylate other substrates, which promote the initiation of replication complex assembly, and stimulate DNA synthesis.[27−31] Furthermore, appropriately timed deactivation of E2F is critical for S-phase progression, and this is also, at least partly, mediated by cyclin A/CDK2. E2F-1 forms stable complexes with cyclin A/CDK2, which phosphorylate bound DP-1, resulting in inhibition of DNA-binding by E2F-1. If E2F-1 activity is allowed to persist inappropriately into S phase, as might be the case in

the presence of a CDK2 inhibitor, the result is S-phase arrest and/or apoptosis.[3] Completion of S phase must also be coordinated with the onset of mitosis, a process controlled by cyclin B-dependent kinases. Cyclin B1 protein levels increase prior to the onset of mitosis due to inactivation of the proteolytic anaphase promoting complex (APC). The mechanism of APC inactivation in turn involves cyclin A/CDK2-dependent phosphorylation of its activating subunit, cdh1.[32] Consequently, the failure of cells treated with compound **32** to progress through S phase, or to accumulate cyclin B1, are an indication of efficient cellular CDK2 inhibition. Additionally, there may be a role for inhibition of other CDKs, particularly CDK9, which is inhibited by compound **32** with similar potency as CDK2. Previous reports have suggested that roscovitine[33] and flavopiridol,[34] i.e. CDK inhibitors with similar selectivity profiles, may inhibit general RNA synthesis by blocking the phosphorylation of the carboxy-terminal domain (CTD) of RNA polymerase II. Positive transcription elongation factor b (P-TEFb), which is comprised of CDK9/cyclin T1 or T2 complexes, phosphorylates the CTD of RNA polymerase II, an event which is essential for the transition from transcriptional initiation to elongation in human cells. Progression through the cell cycle would be affected by the lack of transcription of essential genes as a result of the inhibition of CTD phosphorylation.

To look at the effect of compound **32** on unsynchronized cells, HeLa (a cervical carcinoma cell line) cells were incubated for 24 h with 0.1 or 0.5 μM compound **32** and then stained to reveal tubulin (anti-α-tubulin
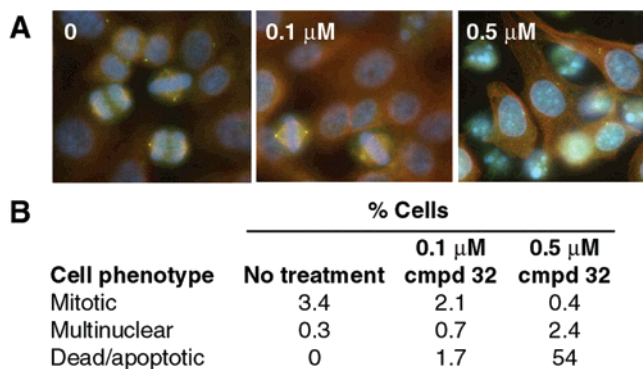
Figure 5. Compound **32** reduces mitotic index and induces cell death in unsynchronized cultured HeLa cells. (A) Cells treated for 24 h with two concentrations of compound **32** were stained with DAPI (blue), anti-α-tubulin (red), and anti-γ-tubulin (green). (B) Percentages of mitotic, multinuclear, and dying cells with fragmented nuclei.

antibody), centrosomes (anti-γ-tubulin antibody), and DNA (DAPI) (Figure 5A). In each sample >1000 cells were counted and the mitotic index was determined by calculating the percentage of cells observed to be in mitosis (prophase, metaphase, anaphase, or telophase, Figure 5B). There was a decrease in mitotic index after drug treatment, suggesting that unsynchronized cells are also unable to enter mitosis and supporting the previous observation that cells are arrested at an earlier point in the cycle. There was also a large increase in cell death after treatment of HeLa cells with 0.5 μM compound **32** (Figure 5B), consistent with apoptosis being triggered by inappropriate E2F-1 activity. A549 cells treated the same way showed a similar reduction of mitotic cells, but not the massive increase in cell death (results not shown) seen with HeLa. This may indicate differences between tumor cell lines in whether their response to S-phase delay results in S-phase arrest or apoptosis.

Conclusions. We have developed the 2-anilino-4-(thiazol-5-yl)pyrimidine CDK inhibitor pharmacophore using structure-based design methods. A prototype compound from the series (**32**) with particularly high biochemical potency against CDKs 2 and 9 was used to demonstrate a cellular mode of action in human tumor cell lines consistent with inhibition of functions of these kinase complexes. We are currently evaluating selected compounds using in vivo tumor efficacy models, as well as further optimizing the pharmaceutical properties in analogues of the inhibitor compound group discussed here.

Experimental Methods

Anhydrous reaction solvents and other reagents were obtained from commercial sources and were used without further purification. Melting points were determined with a Leica testo-720 electrothermometer instrument and are uncorrected. NMR spectra were obtained using Bruker DPX-300 or Varian INOVA-500 instruments. Chemical shifts are reported in parts per million relative to internal tetramethylsilane standard. Mass spectra were obtained using a Waters ZQ2000 single quadrupole mass spectrometer with electrospray ionization (ESI). Elemental analyses were performed by the Analytical Group, Department of Chemistry, The University of Edinburgh, UK. Results obtained were within 0.4% of calculated values. Analytical and preparative RP-HPLC was performed using Vydac 218TP54 (250 × 4.6 mm) and 218TP1022

(250 × 22 mm) columns, respectively. Linear gradient elution using H_2O/MeCN systems (containing 0.1% CF_3COOH) at flow rates of 1 mL/min (analytical) and 9 mL/min (preparative) was performed. Purity was assessed by integration of chromatograms ($\lambda = 254$ nm). Silica gel (EM Kieselgel 60, 0.040−0.063 mm, Merck) or ISOLUTE pre-packed columns (Jones Chromatography Ltd. UK) were used for flash chromatography.

3-Dimethylamino-1-(2,4-dimethylthiazol-5-yl)propenone (4a, R = Me). A solution of 1-(2,4-dimethylthiazol-5-yl)ethanone (**3a**, R = Me; 10 g, 64 mmol) in dimethoxymethyl-dimethylamine (10 mL, 8.97 g, 75 mmol) was refluxed under N_2. After 21 h, the mixture was cooled and evaporated to dryness. The solid residue was recrystallized from $^iPr_2O/CH_2$-Cl_2 to afford the product as an orange solid (9.94 g, 79%); mp 96−98 °C. Anal. RP-HPLC: t_R 7.1 min (10−70% MeCN, purity 100%). ^{1}H NMR (CDCl$_3$): δ 2.66 (s, 6H, CH$_3$), 2.70 (s, 6H, CH$_3$), 5.37 (d, 1H, $J = 12.2$ Hz, CH), 7.66 (d, 1H, $J = 12.2$ Hz, CH). ^{13}C NMR (DMSO-d_6): δ 18.19, 19.52, 37.77, 45.19, 94.50, 134.01, 153.62, 154.38, 165.64, 179.93. MS (ESI$^+$) m/z 211.01 (M + H)$^+$. Anal. (C$_{10}$H$_{14}$N$_2$OS) C, H, N.

N'-[5-(3-Dimethylaminoacryloyl)-4-methylthiazol-2-yl]-N,N-dimethylformamidine (4b). A mixture of thiourea (**1**, R = H; 5.18 g, 68 mmol) in MeOH (20 mL) was cooled in an ice bath. Pyridine (2 mL) was added, followed by dropwise addition of 3-chloropenta-2,4-dione (**2**; 9.15 g, 68 mmol). The mixture was allowed to warm to room temperature and was stirred for 4 h. The resulting precipitates were filtered and washed with EtOAc to afford 1-(2-amino-4-methylthiazol-5-yl)ethanone **3b** as a white solid in a quantitative yield. Mp 183−185 °C. Anal. RP-HPLC: t_R 4.8 min (10−70% MeCN, purity 100%). ^{1}H NMR (DMSO-d_6): δ 2.31 (s, 3H, CH$_3$), 2.39 (s, 3H, CH$_3$), 7.88 (s, 1H, NH). ^{13}C NMR (DMSO-d_6): δ 18.81, 30.12, 121.91, 157.77, 171.09, 188.97. MS (ESI$^+$) m/z 156.89 (M + H)$^+$. This material (3.35 g, 21 mmol) was treated with dimethoxymethyl-dimethylamine (4.49 g, 38 mol). After heating at 120 °C for 6 h, the mixture was evaporated to dryness. The residue was triturated with EtOAc, and the precipitates were collected and washed with EtOAc/PE (5:1). The title compound was obtained after crystallization from EtOAc/PE (2:1) as an orange solid (4.4 g, 79%): mp 198−199 °C. Anal. RP-HPLC: t_R 7.1 min (10−70% MeCN, purity 100%). ^{1}H NMR (CDCl$_3$): δ 2.64 (s, 3H, CH$_3$), 3.08 (s, 6H, CH$_3$), 3.11 (s, 6H, CH$_3$), 5.35 (d, 1H, $J = 12.2$ Hz, CH), 7.67 (d, 1H, $J = 12.2$ Hz, CH), 8.23 (s, 1H, CH). ^{13}C NMR (DMSO-d_6): δ 18.78, 35.25, 60.44, 94.62, 126.84, 152.95, 153.48, 157.11, 173.75, 180.15. MS (ESI$^+$) m/z 267.15 (M + H)$^+$. Anal. (C$_{12}$H$_{18}$N$_4$OS) C, H, N.

3-Dimethylamino-1-(4-methyl-2-methylaminothiazol-5-yl)propenone (4c, R = Me). A solution of 3-chloropentane-2,4-dione (**2**; 2.5 g, 19 mmol) in MeOH (10 mL) was treated with methyl thiourea (**1**, R = Me; 1.67 g, 19 mmol) and pyridine (1.5 mL). The mixture was stirred at room temperature for 2 h. Precipitated 1-(4-methyl-2-methylaminothiazol-5-yl)ethanone (**3c**, R = Me; 2.1 g, 65%) was filtered, washed with Et$_2$O, and dried: mp 201−203 °C. Anal. RP-HPLC: t_R 5.5 min (10−70% MeCN, purity 100%). ^{1}H NMR (CDCl$_3$): δ 2.47 (s, 3H, CH$_3$), 2.61 (s, 3H, CH$_3$), 3.18 (s, 3H, CH$_3$). ^{13}C NMR (DMSO-d_6): δ 19.16, 30.05, 31.54, 49.28, 121.78, 158.54, 188.81. MS (ESI$^+$) m/z 170.87 (M + H)$^+$. This material (2.05 g, 12 mmol) was suspended in dimethoxymethyldimethylamine (5.3 mL, 4.80 g, 40 mmol), and the mixture was heated at 120 °C with stirring for 16 h. On cooling, the reaction mixture was evaporated to dryness. The residue was crystallized from EtOAc to afford the title product as an orange solid (1.82 g, 67%): mp 209−211 °C. Anal. RP-HPLC: t_R 7.1 min (10−70% MeCN, purity 100%). ^{1}H NMR (CDCl$_3$): δ 2.55 (s, 3H, CH$_3$), 2.94 (s, 3H, CH$_3$), 3.41 (s, 6H, CH$_3$), 5.30 (d, 1H, $J = 12.2$ Hz, CH), 7.64 (d, 1H, $J = 12.2$ Hz, CH). ^{13}C NMR (DMSO-d_6): δ 18.94, 31.41, 54.99, 94.32, 122.05, 152.96, 153.83, 169.41, 179.89. MS (ESI$^+$) m/z 226.11 (M + H]). Anal. (C$_{10}$H$_{15}$N$_3$OS.MeOH) C, H, N.

3-Dimethylamino-1-(2-(ethylamino)-4-methylthiazol-5-yl)propenone (4c, R = Et). To a solution of ethyl thiourea (5.20 g, 50 mmol) in MeOH (25 mL) were added dropwise pyridine (4 mL) and then 3-chloropenta-2,4-dione (6.73 g, 50

mmol). The mixture was stirred at room temperature for 4 h. The precipitates were collected, filtered, and washed several times with Me$_2$CO to afford 1-(2-(ethylamino)-4-methylthiazol-5-yl)ethanone (**3c**, R = Et) as a white solid (9.2 g, 100%): mp 211−213 °C. ^{1}H NMR (CDCl$_3$): δ 1.17 (t, 3H, *J* = 7.3 Hz, CH$_3$), 2.42 (s, 3H, CH$_3$), 2.54 (s, 3H, CH$_3$), 3.42 (m, 2H, CH$_2$). This material (1.83 g, 10 mmol) was suspended in dimethoxymethyldimethylamine (2 mL, 1.79 g, 15 mmol), and the mixture was heated at 115−120 °C for 22 h. After cooling, the reaction mixture was evaporated to dryness. A minimal amount of EtOAc was added, and the resulting precipitates were filtered. After crystallization from EtOAc/MeOH, the title product was obtained as a light yellow solid (1.61 g, 42%): mp 204−205 °C. Anal. RP-HPLC: t_R 7.3 min (10−70% MeCN, purity 100%). ^{1}H NMR (CDCl$_3$): δ 1.25 (t, 3H, *J* = 6.0 Hz, CH$_3$), 2.49 (s, 3H, CH$_3$), 3.20 (s, 6H, CH$_3$), 3.28 (m, 2H, CH$_2$), 5.35 (d, 1H, *J* = 11.5 Hz, CH), 7.67 (d, 1H, *J* = 11.5 Hz, CH). ^{13}C NMR (DMSO-d_6): δ 14.92, 18.95, 31.41, 54.99, 94.34, 121.81, 152.92, 153.74, 168.49, 179.90. MS (ESI$^+$) *m/z* 240.17 (M + H)$^+$.

3-Dimethylamino-1-(2-allylamino-4-methylthiazol-5-yl)propenone (4c, R = All). A solution of allyl thiourea (**1**, R = All; 3.95 g, 34 mmol) in MeOH (10 mL) was treated with 3-chloropenta-2,4-dione (**2**; 4.58 g, 34 mmol) and pyridine (3 mL). The mixture was refluxed for 20 min, cooled to room temperature, and stirred for 24 h. After concentration, the resulting precipitates were filtered and washed several times with Et$_2$O to afford 1-(2-allylamino-4-methylthiazol-5-yl)ethanone (**3c**, R = All) as a white solid (6.0 g, 90%): mp 136−138 °C. Anal. RP-HPLC: t_R 7.7 min (10−70% MeCN, purity 100%). ^{1}H NMR (DMSO-d_6): δ 2.43 (s, 3H, CH$_3$), 3.89 (m, 2H, CH$_2$), 5.13−5.24 (m, 2H, CH$_2$), 5.84 (m, 1H, CH, NH), 8.84 (sb, 1H, NH). ^{13}C NMR (CDCl$_3$): δ 17.14, 93.95, 115.84, 121.52, 133.64, 153.89, 154.29, 170.04, 181.99. MS (ESI$^+$) *m/z* 197.02 (M + H)$^+$. Anal. (C$_9$H$_{12}$N$_2$OS.2Me$_2$CO) C, H, N. This material (1.24 g, 6 mmol) was treated with dimethoxymethyldimethylamine (5.3 mL, 4.8 g, 40 mmol). After refluxing for 12 h, the mixture was cooled and concentrated. The resulting precipitates were collected and washed with EtOAc/MeOH (10:1) to afford the title product as a light yellow solid (1.0 g, 65%): mp 136−138 °C. Anal. RP-HPLC: t_R 7.7 min (10−70% MeCN, purity 100%). ^{1}H NMR (DMSO-d_6): δ 2.46 (s, 3H, CH$_3$), 3.22 (s, 6H, CH$_3$), 3.87 (m, 2H, CH$_2$), 5.11−5.28 (m, 3H, CH$_2$ & CH), 5.89 (m, 1H, CH), 7.54 (d, 1H, *J* = 12.0 Hz, CH). ^{13}C NMR (DMSO-d_6): δ 18.93, 47.00, 55.03, 94.29, 116.66, 122.28, 135.16, 152.99, 153.42, 168.46, 179.89. MS (ESI$^+$) *m/z* 252.13 (M + H)$^+$. Anal. (C$_{12}$H$_{17}$N$_3$OS.MeOH) C, H, N.

General Procedure for the Preparation of *N*-Phenylguanidine Nitrates (6). To an ice-cooled mixture of the appropriate aniline **5** (25 mmol) in EtOH (6 mL) was added nitric acid (1.8 mL of 70% solution in H$_2$O) dropwise with stirring. After complete addition, cyanamide (5 mL of 50% solution in H$_2$O) was added, and the mixture was heated at 100 °C for 16−18 h under N$_2$. After cooling to room temperature, it was poured into excess Et$_2$O and was basified with aq NaOH solution. The ethereal layer was separated, and the aqueous phase was extracted with Et$_2$O several times. The combined organic phases were washed with brine, dried on MgSO$_4$, filtered, and evaporated. The resulting residue was purified by crystallization or flash chromatography in appropriate mixtures of EtOAc/PE or EtOAc/MeOH.

General Procedure for the Preparation of [4-(Thiazol-5-yl)pyrimidin-2-yl]phenylamines (7). A mixture of 3-(dimethylamino)-1-thiazol-5-yl-propenone (**4**; 1 equiv), the appropriate *N*-phenylguanidine nitrate (**6**; 2 equiv), and NaOH (1 equiv) in 2-methoxyethanol (0.2 mL/mmol) was heated at 125 °C for 22 h under N$_2$. After cooling, the solvent was evaporated and the residue was purified by flash chromatography using appropriate mixtures of EtOAc/hexane as the eluant. The products **7** were further purified by crystallization from EtOAc/MeOH.

4-(2,4-Dimethylthiazol-5-yl)pyrimidin-2-ylamine (8). From 3-(dimethylamino)-1-(2,4-dimethylthiazol-5-yl)propenone (**4a**, R = Me) and guanidine carbonate. Yellow solid (33%): mp 177−178 °C. Anal. RP-HPLC: t_R 8.6 min (0−60% MeCN,

purity 100%). ^{1}H NMR (DMSO-d_6): δ 2.57 (s, 3H, CH$_3$), 2.60 (s, 3H, CH$_3$), 6.66 (bs, 2H, NH$_2$), 6.79 (d, 1H, *J* = 5.3 Hz, Py-H), 8.26 (d, 1H, *J* = 5.5 Hz, Py-H). ^{13}C NMR (DMSO-d_6): δ 18.44, 19.58, 107.20, 131.43, 152.05, 158.91, 159.70, 164.02, 166.41. MS (ESI$^+$) *m/z* 207.21 (M + H)$^+$. Anal. (C$_9$H$_{10}$N$_4$S) C, H, N.

[4-(2,4-Dimethylthiazol-5-yl)-pyrimidin-2-yl]methylamine (9). From 3-(dimethylamino)-1-(2,4-dimethylthiazol-5-yl)propenone (**4a**, R = Me) and *N*-methylguanidine nitrate. Buff solid (60%): mp 112−113 °C. Anal. RP-HPLC: t_R 10.2 min (0−60% MeCN, purity 100%). ^{1}H NMR (DMSO-d_6): δ 2.59 (s, 3H, CH$_3$), 2.79 (s, 3H, CH$_3$), 2.80 (s, 3H, CH$_3$), 6.77 (bs, 1H, NH), 7.11 (bs, 1H, Py-H), 8.29 (bs, 1H, Py-H). ^{13}C NMR (DMSO-d_6): δ 18.50, 19.57, 28.44, 106.77, 131.41, 152.23, 158.66, 159.54, 163.18, 166.43. MS (ESI$^+$) *m/z* 221.27 (M + H)$^+$. Anal. (C$_{10}$H$_{12}$N$_4$S·0.33H$_2$O) C, H, N.

[4-(2,4-Dimethylthiazol-5-yl)-pyrimidin-2-yl]dimethylamine (10). From 3-(dimethylamino)-1-(2,4-dimethylthiazol-5-yl)propenone (**4a**, R = Me) and *N,N*-dimethylguanidine nitrate. Brown solid (57%): mp 75−76 °C. Anal. RP-HPLC: t_R 10.5 min (0−60% MeCN, purity 100%). ^{1}H NMR (DMSO-d_6): δ 2.60 (s, 3H, CH$_3$), 3.11 (s, 6H, CH$_3$), 6.77 (d, 1H, *J* = 5.5 Hz, Py-H), 8.34 (d, 1H, *J* = 5.5 Hz, Py-H). ^{13}C NMR (DMSO-d_6): δ 18.57, 19.57, 37.15, 106.11, 131.47, 152.36, 158.42, 159.37, 162.18, 166.57. MS (ESI$^+$) *m/z* 235.22 (M + H)$^+$.

[4-(2,4-Dimethylthiazol-5-yl)-pyrimidin-2-yl]phenylamine (11). From 3-(dimethylamino)-1-(2,4-dimethylthiazol-5-yl)propenone (**4a**, R = Me) and phenylguanidine nitrate (**6**, R^1 = R^2 = R^3 = H). Pale pink solid (48%): mp 153−155 °C; Anal. RP-HPLC: t_R 17.7 min (0−60% MeCN, purity 100%). ^{1}H NMR (DMSO-d_6): δ 2.61 (s, 3H, CH$_3$), 2.64 (s, 3H, CH$_3$), 6.95 (m, 1H, Ph-H), 7.06 (d, 1H, *J* = 5.0 Hz, Py-H), 7.28 (m, 2H, Ph-H), 7.77 (m, 2H, Ph-H), 8.49 (d, 1H, *J* = 5.5 Hz, Py-H). ^{13}C NMR (DMSO-d_6): δ 18.57, 19.67, 37.15, 109.10, 119.67, 122.25, 129.16, 131.46, 140.98, 152.66, 158.59, 159.73, 160.37, 167.10. MS (ESI$^+$) *m/z* 283.19 (M + H)$^+$. Anal. (C$_{15}$H$_{14}$N$_4$S·0.33H$_2$O) C, H, N.

(2-Chlorophenyl)-[4-(2,4-dimethylthiazol-5-yl)pyrimidin-2-yl]amine (12). From 3-(dimethylamino)-1-(2,4-dimethylthiazol-5-yl)propenone (**4a**, R = Me) and 2-chlorophenylguanidine nitrate (**6**, R^1 = Cl, R^2 = R^3 = H). Pale yellow solid (95%): mp 190−191 °C. Anal. RP-HPLC: t_R 20.3 min (0−60% MeCN, purity 100%). ^{1}H NMR (DMSO-d_6): δ 2.55 (s, 3H, CH$_3$), 2.60 (s, 3H, CH$_3$), 7.04 (d, 1H, *J* = 5.3 Hz, Py-H), 7.16 (m, 1H, Ph-H), 7.34 (m, 1H, Ph-H), 7.49 (m, 1H, Ph-H), 7.76 (m, 1H, Ph-H), 8.43 (d, 1H, *J* = 5.1 Hz, Py-H), 8.85 (bs, 1H, NH). ^{13}C NMR (DMSO-d_6): δ 18.47, 19.63, 109.57, 126.18, 126.74, 128.04, 128.24, 130.12, 130.91, 136.98, 152.95, 158.86, 159.85, 160.77, 167.08. MS (ESI$^+$) *m/z* 316.51 (M + H)$^+$. Anal. (C$_{15}$H$_{13}$ClN$_4$S) C, H, N.

(3-Chlorophenyl)-[4-(2,4-dimethylthiazol-5-yl)pyrimidin-2-yl]amine (13). From 3-(dimethylamino)-1-(2,4-dimethylthiazol-5-yl)propenone (**4a**, R = Me) and 3-chlorophenylguanidine nitrate (**6**, R^1 = H, R^2 = Cl, R^3 = H). Light yellow solid (52%): mp 191−192 °C. Anal. RP-HPLC: t_R 19.8 min (10−70% MeCN, purity 100%). ^{1}H NMR (DMSO-d_6): δ 2.52 (s, 3H, CH$_3$), 2.64 (s, 3H, CH$_3$), 6.99 (m, 1H, Ph-H), 7.13 (d, 1H, *J* = 5.1 Hz, Py-H), 7.30 (m, 1H, Ph-H), 8.04 (s, 1H, Ph-H), 8.55 (d, 1H, *J* = 5.1 Hz, Py-H), 9.88 (bs, 1H, NH). ^{13}C NMR (DMSO-d_6): δ 18.59, 19.69, 109.76, 117.88, 121.67, 130.77, 131.25, 133.70, 142.56, 152.96, 158.62, 159.84, 160.05, 167.08. MS (ESI$^+$) *m/z* 316.51 (M + H)$^+$. Anal. (C$_{15}$H$_{13}$ClN$_4$S) C, H, N.

(4-Chlorophenyl)-[4-(2,4-dimethylthiazol-5-yl)pyrimidin-2yl]amine (14). From 3-(dimethylamino)-1-(2,4-dimethylthiazol-5-yl)propenone (**4a**, R = Me) and 4-chlorophenylguanidine nitrate (**6**, R^1 = R^2 = H, R^3 = Cl). Light yellow solid (30%): mp 291−292 °C. Anal. RP-HPLC: t_R 13.5 min (10−70% MeCN, purity 100%). ^{1}H NMR (DMSO-d_6): δ 2.42 (s, 3H, CH$_3$), 3.08 (s, 3H, CH$_3$), 6.89 (d, 1H, *J* = 5.5 Hz, Py-H), 7.28 (m, 2H, Ph-H), 7.77 (m, 2H, Ph-H), 8.32 (d, 1H, *J* = 5.3 Hz, Py-H), 9.55 (bs, 1H, NH). ^{13}C NMR (DMSO-d_6): δ 19.14, 107.96, 118.57, 120.93, 120.96, 125.25, 128.86, 140.34, 152.96, 158.31, 159.39, 159.92, 169.57. MS (ESI$^+$) *m/z* 318.04 (M + H)$^+$.

(2-Fluorophenyl)-[4-(2,4-dimethylthiazol-5-yl)pyrimidin-2-yl]amine (15). From 3-(dimethylamino)-1-(2,4-dimethylthiazol-5-yl)propenone (**4a**, R = Me) and 2-fluorophenylguanidine nitrate (**6**, R^1 = F, R^2 = R^3 = H). Grey solid (100%): mp 182−183 °C. Anal. RP-HPLC: t_R 17.4 min (10−70% MeCN, purity 100%). ^{1}H NMR (DMSO-d_6): δ 2.56 (s, 3H, CH$_3$), 2.60 (s, 3H, CH$_3$), 7.03 (d, 1H, J = 5.1 Hz, Py-H), 7.15−7.25 (m, 3H, Ph-H), 7.69 (m, 1H, Ph-H), 8.44 (d, 1H, J = 5.3 Hz, Py-H), 9.12 (bs, 1H, NH). ^{13}C NMR (DMSO-d_6): δ 18.46, 19.60, 109.40, 116.20, 124.76, 125.60, 126.10, 127.80, 131.01, 152.86, 154.96, 156.91, 158.82, 159.73, 160.79, 166.99. MS (ESI$^+$) m/z 301.10 (M + H)$^+$. Anal. (C$_{15}$H$_{13}$FN$_4$S·0.5H$_2$O) C, H, N.

(3-Fluorophenyl)-[4-(2,4-dimethylthiazol-5-yl)pyrimidin-2-yl]amine (16). From 3-(dimethylamino)-1-(2,4-dimethylthiazol-5-yl)propenone (**4a**, R = Me) and 3-fluorophenylguanidine nitrate (**6**, R^1 = H, R^2 = F, R^3 = H). Grey solid (69%): mp 205 °C (dec). Anal. RP-HPLC: t_R 18.0 min (10−70% MeCN, purity 100%). ^{1}H NMR (DMSO-d_6): δ 2.63 (s, 3H, CH$_3$), 2.66 (s, 3H, CH$_3$), 6.75 (m, 1H, Ph-H), 7.13 (d, 1H, J = 5.1 Hz, Py-H), 7.30 (m, 1H, Ph-H), 7.48 (m, 1H, Ph-H), 7.81 (m, 1H, Ph-H), 8.55 (d, 1H, J = 5.5 Hz, Py-H), 9.89 (bs, 1H, NH). ^{13}C NMR (DMSO-d_6): δ 18.58, 19.70, 106.00, 108.35, 109.69, 115.28, 130.68, 142.90, 152.89, 158.62, 159.81, 160.09, 162.06, 163.97, 167.25. MS (ESI$^+$) m/z 300.47 (M + H)$^+$. Anal. (C$_{15}$H$_{13}$FN$_4$S) C, H, N.

(4-Fluorophenyl)-[4-(2,4-dimethylthiazol-5-yl)pyrimidin-2-yl]amine (17). From 3-(dimethylamino)-1-(2,4-dimethylthiazol-5-yl)propenone (**4a**, R = Me) and 4-fluorophenylguanidine nitrate (**6**, R^1 = R^2 = H, R^3 = F). Grey solid (89%): mp 199−200 °C. Anal. RP-HPLC: t_R 16.4 min (10−70% MeCN, purity 100%). ^{1}H NMR (DMSO-d_6): δ 2.61 (s, 3H, CH$_3$), 2.63 (s, 3H, CH$_3$), 7.06 (d, 1H, J = 5.2 Hz, Py-H), 7.13 (m, 2H, Ph-H), 7.75 (m, 2H, Ph-H), 8.49 (d, 1H, J = 5.3 Hz, Py-H), 9.66 (bs, 1H, NH). ^{13}C NMR (DMSO-d_6): δ 18.55, 19.65, 109.11, 115.55, 121.35, 121.38, 131.38, 137.34, 152.69, 156.94, 158.60, 158.83, 159.70, 160.28, 167.05. MS (ESI$^+$) m/z 300.41 (M + H)$^+$. Anal. (C$_{15}$H$_{13}$FN$_4$S) C, H, N.

[4-(2,4-Dimethylthiazol-5-yl)pyrimidin-2-yl]-(2-trifluoromethylphenyl)amine (18). From 3-(dimethylamino)-1-(2,4-dimethylthiazol-5-yl)propenone (**4a**, R = Me) and N-(2-trifluoromethylphenyl)guanidine nitrate (**6**, R^1 = CF$_3$, R^2 = R^3 = H). Yellow solid (31%): mp 178−180 °C. Anal. RP-HPLC: t_R 18.6 min (10−70% MeCN, purity 100%). ^{1}H NMR (DMSO-d_6): δ 2.07 (s, 3H, CH$_3$), 2.58 (s, 3H, CH$_3$), 6.99 (d, 1H, J = 5.3 Hz, Py-H), 7.41 (m, 1H, Ph-H), 7.67 (m, 1H, Ph-H), 7.73 (m, 1H, Ph-H), 8.39 (d, 1H, J = 5.3 Hz, Py-H), 8.84 (bs, 1H, NH). ^{13}C NMR (DMSO-d_6): δ 18.55, 19.62, 109.76, 115.32, 118.24, 123.99, 126.16, 130.23, 131.29, 141.84, 153.00, 158.56, 159.88, 160.04, 167.22. MS (ESI$^+$) m/z 351.31 (M + H)$^+$. Anal. (C$_{16}$H$_{13}$F$_3$N$_4$S) C, H, N.

[4-(2,4-Dimethylthiazol-5-yl)pyrimidin-2-yl]-(3-trifluoromethylphenyl)amine (19). From 3-(dimethylamino)-1-(2,4-dimethylthiazol-5-yl)propenone (**4a**, R = Me) and N-(3-trifluoromethylphenyl)guanidine nitrate (**6**, R^1 = H, R^2 = CF$_3$, R^3 = H). Orange solid (60%): mp 194−195 °C. Anal. RP-HPLC: t_R 20.3 min (10−70% MeCN, purity 100%). ^{1}H NMR (DMSO-d_6): δ 2.63 (s, 3H, CH$_3$), 2.64 (s, 3H, CH$_3$), 7.16 (d, 1H, J = 5.3 Hz, Py-H), 7.29 (s, 1H, Ph-H), 7.51 (m, 1H, Ph-H), 8.35 (s, 1H, Ph-H), 8.57 (d, 1H, J = 5.3 Hz, Py-H), 10.03 (s, 1H, NH). ^{13}C NMR (DMSO-d_6): δ 18.39, 19.59, 109.40, 123.50, 125.50, 126.46, 127.05, 130.54, 133.64, 138.06, 152.96, 158.90, 159.79, 161.88, 166.94. MS (ESI$^+$) m/z 350.86. Anal. (C$_{16}$H$_{13}$F$_3$N$_4$S·0.5H$_2$O) C, H, N.

[4-(2,4-Dimethylthiazol-5-yl)pyrimidin-2-yl]-(4-trifluoromethylphenyl)amine (20). From 3-(dimethylamino)-1-(2,4-dimethylthiazol-5-yl)propenone (**4a**, R = Me) and N-(4-trifluoromethylphenyl)guanidine nitrate (**6**, R^1 = R^2 = H, R^3 = CF$_3$). Orange solid (38%): mp 183−185 °C. Anal. RP-HPLC: t_R 21.1 min (10−70% MeCN, purity 100%). ^{1}H NMR (DMSO-d_6): δ 2.73 (s, 3H, CH$_3$), 2.75 (s, 3H, CH$_3$), 7.06 (d, 1H, J = 5.3 Hz, Py-H), 7.28 (s, 1H, Ph-H), 7.40 (bs, 1H, NH), 7.65 (m, 1H, Ph-H), 7.83 (m, 1H, Ph-H), 8.49 (d, 1H, J = 5.3 Hz, Py-H). ^{13}C NMR (DMSO-d_6): δ 47.96, 47.54, 52.60, 91.95, 96.57, 98.20, 99.16, 99.21, 99.28, 100.13, 102.50, 108.08,

113.30, 116.29, 116.50, 120.51. MS (ESI$^+$) m/z 351.42 (M + H)$^+$. Anal. (C$_{16}$H$_{13}$F$_3$N$_4$S) C, H, N.

3-[4-(2,4-Dimethylthiazol-5-yl)pyrimidin-2-ylamino]phenol (21). From 3-(dimethylamino)-1-(2,4-dimethylthiazol-5-yl)propenone (**4a**, R = Me) and N-(3-hydroxyphenyl)guanidine nitrate (**6**, R^1 = R^2 = OH, R^3 = H). Orange solid (36%): mp 235 °C (dec). Anal. RP-HPLC: t_R 12.1 min (10−70% MeCN, purity 100%). ^{1}H NMR (DMSO-d_6): δ 2.62 (s, 3H, CH$_3$), 2.64 (s, 3H, CH$_3$), 6.37 (m, 1H, Ph-H), 7.04 (m, 2H, Py-H & Ph-H), 7.21 (m, 2H, Ph-H), 8.48 (d, 1H, J = 5.1 Hz, Py-H), 9.21 (s, 1H, OH/NH), 9.50 (s, 1H, NH/OH). ^{13}C NMR (DMSO-d_6): δ 18.51, 19.65, 106.98, 109.05, 109.59, 110.76, 129.72, 131.41, 141.97, 152.61, 158.19, 158.67, 159.48, 160.29, 167.16. MS (ESI$^+$) m/z 299.29 (M + H)$^+$.

3-[4-(4-Methyl-2-methylaminothiazol-5-yl)pyrimidin-2-ylamino]phenol (22). From 3-(dimethylamino)-1-(2-methylamino-4-methylthiazol-5-yl)propenone (**4c**, R = Me) and N-(3-hydroxyphenyl)guanidine nitrate (**6**, R^1 = R^2 = OH, R^3 = H). Yellow solid (19%): mp 251 °C (dec). Anal. RP-HPLC: t_R 16.3 min (0−60% MeCN, purity 100%). ^{1}H NMR (DMSO-d_6): δ 2.86 (s, 3H, CH$_3$), 3.24 (s, 3H, CH$_3$), 6.36 (d, 1H, J = 4.9 Hz, Ph-H), 6.89 (d, 1H, J = 5.5 Hz, Py-H), 7.03 (t, 1H, J = 8.7 Hz, Ph-H), 7.24 (bs, 1H, Ph-H), 8.06 (bs, 1H, OH), 8.33 (d, 1H, J = 4.5 Hz, Py-H), 9.22 (s, 1H, NH), 9.31 (s, 1H, NH). ^{13}C NMR (DMSO-d_6): δ 19.33, 31.42, 106.75, 107.45, 109.15, 110.54, 118.49, 129.59, 142.37, 152.92, 158.15, 158.17, 159.33, 160.20, 169.96. MS (ESI$^+$) m/z 314.02 (M + H)$^+$. Anal. (C$_{15}$H$_{15}$N$_5$OS) C, H, N.

3-[4-(2-Ethylamino-4-methylthiazol-5-yl)pyrimidin-2-ylamino]phenol (23). From 3-(dimethylamino)-1-(2-(ethylamino)-4-methylthiazol-5-yl)propenone (**4c**, R = Et) and N-(3-hydroxyphenyl)guanidine nitrate (**6**, R^1 = R^2 = OH, R^3 = H). Light yellow solid. Anal. RP-HPLC: t_R 17.7 min (0−60% MeCN, purity 100%). ^{1}H NMR (DMSO-d_6): δ 1.15 (t, 3H, J = 7.5 Hz, CH$_3$), 2.49 (s, 3H, CH$_3$), 3.25 (m, 2H, CH$_2$), 6.33 (d, 1H, J = 8.3 Hz, Ph-H), 6.86 (d, 1H, J = 5.4 Hz, Py-H), 7.00 (t, 1H, J = 7.7 Hz, Ph-H), 7.21 (m, 2H, Ph-H and OH), 8.10 (t, 1H, J = 5.9 Hz, Ph-H), 8.29 (d, 1H, J = 5.4 Hz, Py-H), 9.19 (s, 1H, NH), 9.28 (s, 1H, NH). ^{13}C NMR (DMSO-d_6): δ 14.97, 19.34, 106.72, 106.74, 107.47, 109.13, 110.53, 118.21, 129.58, 142.38, 152.85, 158.15, 159.34, 160.20, 169.02. MS (ESI$^+$) m/z 328.05 (M + H)$^+$.

4-[4-(2,4-Dimethyl-thiazol-5-yl)-pyrimidin-2-ylamino]phenol (24). From 3-(dimethylamino)-1-(2,4-dimethylthiazol-5-yl)propenone (**4a**, R = Me) and N-(4-hydroxyphenyl)guanidine nitrate (**6**, R^1 = R^2 = H, R^3 = OH). Orange solid (81%): mp 230 °C (dec). Anal. RP-HPLC: t_R 10.9 min (10−70% MeCN, purity 100%). ^{1}H NMR (CDCl$_3$): δ 2.59 (s, 3H, CH$_3$), 2.62 (s, 3H, CH$_3$), 6.69 (d, 1H, J = 8.8 Hz, Ph-H), 6.96 (d, 1H, J = 5.1 Hz, Py-H), 7.47 (d, 1H, J = 8.9 Hz, Ph-H), 8.41 (d, 1H, J = 5.1 Hz, Py-H), 9.03 (bs, 1H, NH/OH), 9.29 (bs, 1H, OH/NH). ^{13}C NMR (DMSO-d_6): δ 18.52, 19.62, 108.25, 115.60, 121.96, 131.57, 132.48, 152.42, 153.13, 158.54, 159.58, 160.63, 166.85. MS (ESI$^+$) m/z 299.23 (M + H)$^+$. Anal. (C$_{15}$H$_{14}$N$_4$OS·0.33H$_2$O) C, H, N.

4-[4-(4-Methyl-2-methylaminothiazol-5-yl)pyrimidin-2-ylamino]phenol (25). From 3-(dimethylamino)-1-(2-methylamino-4-methylthiazol-5-yl)propenone (**4c**, R = Me) and N-(4-hydroxyphenyl)guanidine nitrate (**6**, R^1 = R^2 = H, R^3 = OH). Orange solid (60%): mp 213-214 °C. Anal. RP-HPLC: t_R 9.7 min (10−70% MeCN, purity 100%). ^{1}H NMR (DMSO-d_6): δ 2.53 (s, 3H, CH$_3$), 2.98 (s, 3H, CH$_3$), 6.77 (d, 1H, J = 8.8 Hz, Ph-H), 6.87 (d, 1H, J = 5.6 Hz, Py-H), 7.44 (d, 1H, J = 8.8 Hz, Ph-H), 8.21 (d, 1H, J = 5.4 Hz, Py-H). ^{13}C NMR (DMSO-d_6): δ 19.29, 31.36, 106.71, 115.54, 116.84, 118.69, 121.62, 128.22, 132.87, 152.77, 152.78, 158.27, 159.23, 160.39, 169.81. MS (ESI$^+$) m/z 313.61.

4-[4-(2-Amino-4-methylthiazol-5-yl)pyrimidin-2-ylamino]phenol (26). From N′-[5-(3-dimethylaminoacryloyl)-4-methylthiazol-2-yl]-N,N-dimethylformamidine (**4b**) and N-(4-hydroxyphenyl)guanidine nitrate (**6**, R^1 = R^2 = H, R^3 = OH). Yellow solid (43%): mp 212−213 °C. Anal. RP-HPLC: t_R 10.5 min (0−60% MeCN, purity 100%). ^{1}H NMR (DMSO-d_6): δ 2.40, (s, 3H, CH$_3$), 6.65 (m, 2H, Ph-H), 6.77 (d, 1H, J = 5.5 Hz, Py-

H), 7.43 (bs, 2H, NH$_2$), 7.48 (d, 1H, $J = 8.9$ Hz, Ph-H), 8.23 (d, 1H, $J = 5.3$ Hz, Py-H), 9.01 (bs, 1H, NH$_2$), 9.05 (bs, 1H, OH). ^{13}C NMR (DMSO-d_6): δ 19.08, 106.75, 106.76, 115.52, 115.54, 118.92, 121.55, 132.83, 152.31, 152.83, 158.27, 158.28, 159.27, 160.38, 169.40. MS (ESI$^+$) m/z 300.07 (M + H)$^+$.

2-[N−(3-Nitrophenyl)]-4-(2,4-dimethylthiazol-5-yl)py-rimidineamine (27). From 3-(dimethylamino)-1-(2,4-dimethylthiazol-5-yl)propenone (**4a**, R = Me) and 3-nitrophenylguanidine nitrate (**6**, R^1 = H, R^2 = NO$_2$, R^3 = H). Yellow solid (72%): mp 176−178 °C. Anal. RP-HPLC: t_R 18.2 min (10−70% MeCN, purity 100%). ^{1}H NMR (CDCl$_3$): δ 2.64 (s, 3H, CH$_3$), 2.65 (s, 3H, CH$_3$), 7.19 (d, 1H, $J = 5.3$ Hz, Ph-H), 7.58 (t, 1H, $J = 8.2$ Hz, Ph-H), 7.80 (m, 1H, Ph-H), 8.05 (m, 1H, Ph-H), 8.60 (d, 1H, $J = 5.2$ Hz, Py-H), 8.91 (m, 1H, Ph-H), 10.20 (br. s, 1H, NH). ^{13}C NMR (DMSO-d_6): δ 18.58, 19.66, 110.04, 113.12, 116.41, 125.36, 130.36, 131.18, 142.33, 148.80, 153.10, 158.65, 159.81, 159.87, 167.28. MS (ESI$^+$) m/z 327.62 (M + H)$^+$. Anal. (C$_{15}$H$_{13}$N$_5$O$_2$S) C, H, N.

[4-(2,4-Dimethylthiazol-5-yl)-pyrimidin-2-yl]methyl-(3-nitrophenyl)amine (28). Compound **27** (0.5 g, 1.53 mmol) was dissolved in anhydrous DMF (5 mL), and sodium hydride (95%, 0.043 g, 1.68 mmol) was added in portions. The mixture was stirred for 30 min before the dropwise addition of iodomethane (0.115 mL, 1.68 mmol). After stirring for 1 h, the mixture was poured into water (70 mL) and extracted with EtOAc. The extract was washed with brine, dried on Na$_2$SO$_4$ and the solvent was evaporated to leave a yellow residue, which was purified by flash chromatography (4:1 EtOAc/heptane). Recrystallization from EtOAc afforded the title product as yellow crystals (0.33 g, 62%): mp 145−146 °C. Anal. RP-HPLC: t_R 20.1 min (0−60% MeCN, purity 100%). ^{1}H NMR (CDCl$_3$): δ 2.53 (s, 3H, CH$_3$), 2.59 (s, 3H, CH$_3$), 3.56 (s, 3H, CH$_3$), 7.05 (d, 1H, $J = 4.9$ Hz, Py-H), 7.67 (t, 1H, $J = 8.3$ Hz, Ph-H), 7.88 (m, 1H, Ph-H), 8.04 (d, 1H, $J = 8.3$ Hz, Ph-H), 8.28 (s, 1H, Ph-H), 8.46 (d, 1H, $J = 5.4$ Hz, Py-H). ^{13}C NMR (DMSO-d_6): δ 18.50, 19.61, 38.29, 109.25 120.22, 121.46, 130.48, 130.51, 133.28, 146.56, 148.56, 153.09, 158.60, 159.56, 161.22, 167.17. MS (ESI$^+$) m/z 342.17 (M + H)$^+$. Anal. (C$_{15}$H$_{13}$N$_5$O$_2$S) C, H, N.

[4-(2-N,N-Dimethylamino-4-methylthiazol-5-yl)pyrimidin-2-yl]-(3-nitrophenyl)amine (29). From 3-(dimethylamino)-1-(2-N,N-dimethylamino-4-methylthiazol-5-yl)propenone (**4a**, R = NMe$_2$) and 3-nitrophenylguanidine nitrate (**6**, R^1 = H, R^2 = NO$_2$, R^3 = H). Yellow solid (47%): mp 250−252 °C. Anal. RP-HPLC: t_R 14.8 min (10−70% MeCN, purity 100%). ^{1}H NMR (CDCl$_3$): δ 2.52 (s, 3H, CH$_3$), 3.11 (s, 6H, CH$_3$), 7.02 (d, 1H, $J = 5.4$ Hz, Py-H), 7.54 (m, 1H, Ph-H), 7.79 (m, 1H, Ph-H), 7.97 (m, 1H, Ph-H), 8.40 (d, 1H, $J = 5.3$ Hz, Py-H), 8.45 (s, 1H, NH), 9.05 (m, 1H, Ph-H), 10.02 (s, 1H, NH). ^{13}C NMR (DMSO-d_6): δ 19.43, 108.08, 112.78, 116.19, 119.75, 125.32, 130.32, 142.65, 148.94, 154.09, 158.59, 159.12, 159.70, 170.41. MS (ESI$^+$) m/z 357.05 (M + H)$^+$.

[4-(4-Methyl-2-methylaminothiazol-5-yl)pyrimidin-2-yl](3-nitrophenyl)amine (30). From 3-(dimethylamino)-1-(2-methylamino-4-methylthiazol-5-yl)propenone (**4c**, R = Me) and 3-nitrophenylguanidine nitrate (**6**, R^1 = H, R^2 = NO$_2$, R^3 = H). Orange solid (22%): mp 302−304 °C. Anal. RP-HPLC: t_R 14.8 min (10−70% MeCN, purity 100%). ^{1}H NMR (CDCl$_3$): δ 2.88 (s, 3H, CH$_3$), 3.09 (s, 3H, CH$_3$), 7.02 (d, 1H, $J = 5.4$ Hz, Py-H), 7.56 (t, 1H, $J = 7.8$ Hz, Ph-H), 7.79 (m, 1H, Ph-H), 8.02 (m, 1H, Ph-H), 8.17 (bs, 1H, NH), 8.42 (d, 1H, $J = 5.2$ Hz, Py-H), 8.98 (m, 1H, Ph-H). ^{13}C NMR (DMSO-d_6): δ 19.36, 31.64, 108.33, 112.94, 116.10, 118.31, 125.26, 130.27, 142.67, 148.86, 153.79, 158.36, 159.34, 159.72, 170.50. MS (ESI$^+$) m/z 342.98 (M + H)$^+$. Anal. (C$_{15}$H$_{14}$N$_6$O$_2$S·1.5H$_2$O) C, H, N.

[4-(2-Allylamino-4-methylthiazol-5-yl)pyrimidin-2-yl]-(3-nitrophenyl)amine (31). From 3-(dimethylamino)-1-(2-allylamino-4-methylthiazol-5-yl)propenone (**4c**, R = All) and 3-nitrophenylguanidine nitrate (**6**, R^1 = H, R^2 = NO$_2$, R^3 = H); orange solid (33%): mp 307−308 °C. Anal. RP-HPLC: t_R 13.3 min (10−70% MeCN, purity 100%). ^{1}H NMR (CDCl$_3$): δ 2.47 (s, 3H, CH$_3$), 3.89 (m, 1H, CH), 5.13 (m, 1H, CH), 5.24 (m, 1H, CH), 5.88 (m, 1H, CH), 6.99 (d, 1H, $J = 5.7$ Hz, Py-

H), 7.54 (t, 1H, $J = 8.2$ Hz, Ph-H), 7.77 (m, 1H, Ph-H), 8.40 (d, 1H, $J = 5.5$ Hz, Py-H), 8.85 (m, 1H, Ph-H), 9.90 (bs, 1H, NH). MS (ESI$^+$) m/z 369.52 (M + H)$^+$.

[4-(2-Amino-4-methylthiazol-5-yl)pyrimidin-2-yl](3-nitrophenyl)amine (32). From 3-(dimethylamino)-1-(2-amino-4-methylthiazol-5-yl)propenone (**4c**, R = H) and 3-nitrophenylguanidine nitrate (**6**, R^1 = H, R^2 = NO$_2$, R^3 = H); Light yellow solid (80%): mp 270−272 °C; Anal. RP-HPLC: t_R 13.5 min (10−70% MeCN, purity 100%). ^{1}H NMR (CDCl$_3$): δ 2.50 (s, 3H, CH$_3$), 6.98 (d, 1H, $J = 5.5$ Hz, Py-H), 7.61 (m, 2H, Ph-H), 7.79 (m, 1H, Ph-H), 8.10 (m, 1H, Ph-H), 8.40 (d, 1H, $J = 5.4$ Hz, Py-H), 8.82 (bs, 2H, NH$_2$). ^{13}C NMR (DMSO-d_6): δ 19.07, 108.72, 113.10, 116.10, 118.30, 125.23, 130.30, 142.62, 148.77, 153.18, 158.33, 159.50, 159.72, 169.75. MS (ESI$^+$) m/z 329.44 (M + H)$^+$; Anal. (C$_{14}$H$_{12}$N$_6$O$_2$S.HCl) C, H, N.

[4-(4-Methyl-2-pyridin-2-ylthiazol-5-yl)pyrimidin-2-yl]-(3-nitrophenyl)amine (33). To a solution of thionicotinamide (5.02 g, 38 mmol) and pyridine (3.0 g, 38 mmol) in MeOH (10 mL) was added 3-chloropenta-2,4-dione (5.12 g, 38 mmol) dropwise. After heating at 75 °C for 4 h the mixture was concentrated. The resulting precipitates were collected and washed with EtOAc several times to afford a yellow solid of 1-(4-methyl-2-pyridin-3-ylthiazol-5-yl)ethanone (4.33 g, 52%). An aliquot of this material (2.0 g, 9.2 mmol) was treated with dimethoxymethyldimethylamine (4 mL, 30 mmol) at 80 °C for 22 h. The mixture was concentrated and the resulting precipitates were collected and washed with EtOAc/PE (1:5) several times. The dark brown residue was crystallized from EtOAc/PE (1:2) to afford 3-(dimethylamino)-1-(4-methyl-2-pyridin-3-ylthiazol-5-yl)propenone (2.05 g, 82%). ^{1}H NMR (CDCl$_3$): δ 2.94 (s, 3H, CH$_3$), 2.96 (s, 3H, CH$_3$), 3.50 (s, 3H, CH$_3$), 5.48 (d, 1H, $J = 12.0$ Hz, CH), 7.38 (m, 1H, pyridyl-H), 7.77 (d, 1H, $J = 12.1$ Hz, CH), 8.28 (m, 1H, pyridyl-H), 8.66 (m, 1H, pyridyl-H), 9.16 (m, 1H, pyridyl-H). ^{13}C NMR (DMSO-d_6): δ 18.49, 37.93, 45.34, 55.02, 94.30, 124.94, 129.36, 134.29, 135.85, 147.59, 151.87, 154.88, 163.16, 179.42.

The title product was obtained from 3-(dimethylamino)-1-(4-methyl-2-pyridin-3-ylthiazol-5-yl)propenone (0.27 g, 1.0 mmol) and 3-nitrophenylguanidine nitrate (0.24 g, 1.0 mmol; **6**, R^1 = H, R^2 = NO$_2$, R^3 = H) as yellow crystals (0.15 g, 39%): mp 215−217 °C. Anal. RP-HPLC: t_R 20.2 min (10−70% MeCN, purity 100%). ^{1}H NMR (CDCl$_3$): δ 2.82 (s, 3H, CH$_3$), 7.24 (d, 1H, $J = 5.2$ Hz, Py-H), 7.53 (m, 2H, pyridyl-H), 7.82 (m, 1H, pyridyl-H), 8.35 (m, 1H, pyridyl-H), 8.62 (d, 1H, $J = 5.4$ Hz, Py-H), 8.68 (m, 1H, Ar−H), 9.21 (m, 2H, pyridyl-H), 10.24 (sb, 1H, NH). ^{13}C NMR (DMSO-d_6): δ 18.89, 55.06, 110.00, 113.06, 116.64, 119.44, 125.05, 125.55, 129.33, 139.49, 131.17, 131.91, 142.26, 147.63, 148.92, 152.13, 156.54, 159.89, 164.54. MS (ESI$^+$) 391.02 [M + H]$^+$; Anal. (C$_{19}$H$_{14}$N$_6$O$_2$S) C, H, N.

[4-(2,4-Dimethylthiazol-5-yl)pyrimidin-2-yl](4-nitrophenyl)amine (34). From 3-(dimethylamino)-1-(2,4-dimethylthiazol-5-yl)propenone (**4a**, R = Me) and 4-nitrophenylguanidine nitrate (**6**, R^1 = H, R^2 = H, R^3 = NO$_2$). Grey solid: mp 302−304 °C. Anal. RP-HPLC: t_R 19.97 min (10−70% MeCN, purity 100%). ^{1}H NMR (CDCl$_3$): δ 2.66 (s, 3H, CH$_3$), 2.68 (s, 3H, CH$_3$), 7.28 (d, 1H, $J = 5.2$ Hz, Py-H), 8.05 (d, 2H, $J = 9.3$ Hz, Ph-H), 8.23 (d, 2H, $J = 9.3$ Hz, Ph-H), 8.64 (d, 1H, $J = 5.3$ Hz, Py-H), 10.49 (sb, 1H, NH). ^{13}C NMR (DMSO-d_6): δ 18.61, 19.70, 110.00, 110.91, 118.53, 125.66, 125.67, 131.02, 141.18, 147.65, 153.30, 158.84, 159.62, 159.97, 167.62. MS (ESI$^+$) m/z 328.08 [M + H]$^+$.

N-[4-(2,4-Dimethylthiazol-5-yl)pyrimidin-2-yl]benzene-1,3-diamine (35). Compound **27** (0.5 g, 1.53 mmol) was suspended in EtOH (5 mL) and glacial acetic acid (2.5 mL). The mixture was heated to reflux, and iron powder (325 mesh, 0.85 g, 15.3 mmol) was added in potions. Heating was continued for 30 min, and then the hot mixture was filtered through a pad of Celite. The filtrate was cooled, evaporated, treated with saturated aq NaHCO$_3$ solution (75 mL), and extracted with EtOAc. The extract was washed with brine, dried on Na$_2$SO$_4$, and filtered. The solvent was evaporated to leave an orange solid, which was purified by flash chromatography (50:1 CH$_2$Cl$_2$:MeOH.). Crystallization from EtOAc afforded the title product as pale yellow crystals (211 mg,

46%): mp 163–164 °C. Anal. RP-HPLC: t_R 10.8 min (0–60% MeCN, purity 98%). ^{1}H NMR (DMSO-d_6): δ 2.61 (s, 3H, CH₃), 2.63 (s, 3H, CH₃), 4.92 (bs 2H, NH₂), 6.20 (d, 1H, J = 8.3 Hz, Ph-H), 6.90–6.92 (m, 2H, Py-H and Ph-H), 7.00–7.01 (m, 2H, Ph-H), 8.45 (d, 1H, J = 4.9 Hz, Py-H), 9.32 (bs, 1H, NH). ^{13}C NMR (DMSO-d_6): δ 18.55, 19.67, 105.61, 108.20, 108.68, 108.84, 129.38, 131.53, 141.49, 149.44, 152.53, 158.56, 159.56, 160.52, 167.00. MS (ESI⁺) m/z 298.20 (M + H)⁺. Anal. ($C_{15}H_{15}N_5S$) C, H, N.

3-[4-(2,4-Dimethylthiazol-5-yl)pyrimidin-2-ylamino]-benzonitrile (36). From 3-(dimethylamino)-1-(2,4-dimethylthiazol-5-yl)propenone (**4a**, R = Me) and *N*-(3-cyanophenyl)-guanidine nitrate (**6**, R¹ = H, R² = CN, R³ = H). Light yellow crystals (28%): mp 162–163 °C. Anal. RP-HPLC: t_R 17.1 min (10–70% MeCN, purity 97%). ^{1}H NMR (CDCl₃): δ 2.59 (s, 3H, CH₃), 2.60 (s, 3H, CH₃), 7.12 (d, 1H, J = 5.0 Hz, Py-H), 7.35 (m, 1H, Ph-H), 7.45 (t, 1H, J = 8.0 Hz, Ph-H), 7.93 (m, 1H, Ph-H), 8.28 (bs, 1H, NH), 8.53 (d, 1H, J = 5.0 Hz, Py-H). ^{13}C NMR (DMSO-d_6): δ 18.59, 19.68, 110.08, 112.06, 119.75, 121.95, 124.00, 125.42, 130.62, 141.91, 153.08, 158.67, 159.90, 159.94, 167.28. MS (ESI⁺) m/z 308.13 (M + H)⁺.

***N*-[4-(2,4-Dimethylthiazol-5-yl)pyrimidin-2-yl]*N,N*-dimethylbenzene-1,4-diamine (37).** From 3-(dimethylamino)-1-(2,4-dimethylthiazol-5-yl)propenone (**4a**, R = Me) and *N,N*-dimethylaminophenyl guanidine nitrate (**6**, R¹ = H, R² = H, R³ = NMe₂). Yellow crystals (72%): mp 236–238 °C. Anal. RP-HPLC: t_R 11.2 min (0–60% MeCN, purity 97%). ^{1}H NMR (DMSO-d_6): δ 2.60 (s, 3H, CH₃), 2.62 (s, 3H, CH₃), 2.82 (s, 6H, CH₃x2), 6.70 (d, 1H, J = 8.8 Hz, Ph-H), 6.94 (d, 1H, J = 5.3 Hz, Py-H), 7.53 (d, 1H, J = 9.0 Hz, Ph-H), 8.40 (d, 1H, J = 5.3 Hz, Py-H), 9.27 (s, 1H, NH). ^{13}C NMR (CDCl₃): δ 16.47, 17.71, 39.52, 106.51, 111.77, 120.38, 127.53, 129.73, 145.76, 150.50, 156.83, 157.40, 158.75, 165.03. MS (ESI⁺) m/z 326.20 (M + NH)⁺. Anal. ($C_{17}H_{19}N_5S$·0.15H₂O) C, H, N.

***N*⁴-[4-(2,4-Dimethylthiazol-5-yl)pyrimidin-2-yl]*N*¹,*N*¹-dimethyl-2-nitrobenzene-1,4-diamine (38).** Nitric acid (69%, 24 μL, 0.36 mmol) was added dropwise to acetic anhydride (1 mL) at room-temperature, keeping the internal temperature below 25 °C. The mixture was stirred at room temperature for 15 min before cooling to −5 °C in an ice–methanol bath. Compound **38** (50 mg, 0.15 mmol) in acetic anhydride (1 mL) was added dropwise to the cooled solution of acetyl nitrate. After stirring with cooling for 1 h and a further 2 h at room temperature, the mixture was poured into ice–water (20 mL) and the pH was adjusted to 7–8 by the addition of saturated aq NaHCO₃ solution. The mixture was extracted with EtOAc and washed with brine, dried on MgSO₄, and filtered. The solvent was evaporated, and the residue was purified by flash chromatography (heptane/EtOAc) to afford the title product as a pale reddish solid (32 mg, 57%). Anal. RP-HPLC: t_R 12.7min (10–70% MeCN, purity >95%): mp 192–194 °C. ^{1}H NMR (DMSO-d_6): δ 2.61 (s, 3H, CH₃), 2.63 (s, 3H, CH₃), 2.74 (s, 6H, CH₃), 7.07 (d, 1H, J = 5.5 Hz, Py-H), 7.22 (d, 1H, J = 9.0 Hz, Ph-H), 7.77 (dd, 1H, J = 8.7, 2.7 Hz, Ph-H), 8.38 (d, 1H, J = 2.7 Hz), 8.51 (d, 1H, J = 5.1 Hz, Py-H), 9.79 (bs, 1H, NH). ^{13}C NMR (CDCl₃): δ 18.55, 19.68, 43.56, 109.30, 115.73, 120.53, 125.38, 131.32, 133.38, 140.65, 141.38, 152.87, 159.80, 159.81, 160.07, 167.11. MS (ESI⁺) m/z 393.32 (M + Na). Anal. ($C_{17}H_{18}N_6O_2S$) C, H, N.

In an alternative preparation, 4-fluoro-3-nitroaniline (20 g, 128 mmol) was dissolved in ethanol (300 mL), and dimethylamine (5.6 M solution in ethanol, 360 mL, 2.02 mol) was added in a steady stream. After refluxing for 18 h, the reaction mixture was cooled and water (100 mL) was added. The ethanol was removed by evaporation, and the residue was extracted with ether (3 × 100 mL). The combined organics were washed with brine and filtered, and the solvent was evaporated to give 4-(dimethylamino)-3-nitroaniline (22.8 g) as black oil. This was dissolved in ethanol (80 mL), and nitric acid (69%, 18.5 mL, 22.1 mmol) was added dropwise, followed by cyanamide (50% w/v in water, 37 mL, 476 mmol). The mixture was heated at reflux for 18 h. On cooling, the mixture was poured into ether (1 L). The ethereal supernatant was decanted, and the residue was treated with propan-2-ol,

followed by ether to give 19.0 g of 4-*N,N*-dimethylamino-3-nitrophenylguanidine nitrate (**6**, R¹ = H, R² = NO₂, R³ = NMe₂) as a tan solid. This was stirred with potassium carbonate (15.04 g, 108.8 mmol) in 2-methoxyethanol (250 mL) for 10 min before addition of 3-(dimethylamino)-1-(2,4-dimethylthiazol-5-yl)propenone (**4a**, R = Me, 9.53 g, 45.33 mmol). The mixture was heated at 125 °C for 18 h, then concentrated, diluted with EtOAc, filtered through a pad of silica, and evaporated to leave dark oil, which was purified by flash chromatography (EtOAc). Recrystallization from toluene yielded the title product as a reddish solid (7.3 g, 43%).

2-Chloro-*N*⁴-[4-(2,4-dimethylthiazol-5-yl)pyrimidin-2-yl]-*N*¹,*N*¹-dimethylbenzene-1,4-diamine (39). A solution of 3-chloro-4-fluoronitrobenzene (3.0 g, 17.1 mmol), dimethylamine hydrochloride (1.53 g, 18.8 mmol), and potassium carbonate (4.96 g, 35.9 mmol) in dimethyl sulfoxide (20 mL) was heated in a sealed tube at 105 °C for 18 h. On cooling, the reaction mixture was poured into water (200 mL) and was extracted with EtOAc. The extract was washed with brine, dried on MgSO₄, filtered, and evaporated to afford 3.47 g of 3-chloro-4-(dimethylamino)nitrobenzene as a yellow solid. An aliquot (3.4 g, 16.95 mmol) of this material was dissolved in of ethanol/acetic acid (20 mL) with warming. Iron powder (325 mesh, 9.5 g, 170 mmol) was added in portions. The mixture was then heated on a steam bath for 30 min, cooled and filtered through a pad of Celite, and the filtratewas evaporated to give 3.33 g of 3-chloro-4-(dimethylamino)aniline as a dark solid. A solution of this material in ethanol (10 mL) was treated with nitric acid (69%, 2.6 mL, 40.6 mmol) dropwise, followed by cyanamide (50% solution in water, 5.3 mL, 67.78 mmol). After heating for 18 h at reflux, the reaction mixture was cooled to room temperature, poured into ether (100 mL), and basified with sodium hydroxide solution (2 M, 100 mL). The ethereal layer was separated, and the aqueous phase was extracted with ether. The combined organic phases were washed with brine, dried on MgSO₄, filtered, and evaporated to give dark-brown oil, which solidified on standing to afford of 4-*N,N*-dimethylamino-3-chlorophenylguanidine nitrate (1.6 g, 34%; **6**, R¹ = H, R² = Cl, R³ = NMe₂). ^{1}H NMR (DMSO-d_6): δ 2.71 (s, 6H, CH₃), 7.12 (dd, 1H, J = 8.5, 2.4 Hz, Ph-H), 7.18 (d, 1H, J = 8.8 Hz, Ph-H), 7.25 (d, 1H, J = 2.4 Hz, Ph-H), 7.57 (bs, 4H, NH).

In an alternative preparation 3-chloro-4-fluoronitrobenzene (5.0 g, 28.48 mmol) was dissolved in ethanol (150 mL) and dimethylamine (5.6 M solution in ethanol, 80 mL, 448 mmol) was added in a steady stream. The mixture was heated overnight at reflux. It was concentrated in vacuo and water was added. The resulting precipitate was filtered, washed with water, and dried under vacuum at 40 °C to afford of 3-chloro-4-(dimethylamino)nitrobenzene (5.65 g) as a yellow solid.

The title product was obtained 3-(dimethylamino)-1-(2,4-dimethylthiazol-5-yl)propenone (**4a**, R = Me) and 4-*N,N*-dimethylamino-3-chlorophenyl guanidine nitrate (**6**, R¹ = H, R² = Cl, R³ = NMe₂): mp 131–132 °C; RP-HPLC: t_R 9.4 min (10–70% MeCN, purity > 95%). ^{1}H NMR (DMSO-d_6): δ 2.95 (s, 3H, CH₃), 2.97 (s, 3H, CH₃), 3.00 (s, 6H, CH₃), 7.38 (d, 1H, J = 5.2 Hz, Py-H), 7.45 (d, 1H, J = 8.9 Hz, Ph-H), 7.93 (m, 1H, Ph-H), 8.29 (s, 1H, Ph-H), 8.82 (d, 1H, J = 5.2 Hz, Py-H). ^{13}C NMR (DMSO-d_6): δ 18.58, 19.68, 44.35, 109.16, 118.96, 121.08, 121.16, 127.87, 131.39, 136.73, 144.82, 152.77, 158.56, 159.74, 160.12, 167.08. MS (ESI⁺) m/z 359.94 (M). Anal. ($C_{17}H_{18}ClN_5S$) C, H, N.

***N*-[4-(2-Amino-4-methyl-thiazol-5-yl)-pyrimidin-2-yl]-*N,N*-dimethylbenzene-1,4-diamine (40).** From *N*-[5-(3-dimethylaminoacryloyl)-4-methylthiazol-2-yl]-*N,N*-dimethylformamidine (**4b**) and *N,N*-dimethylaminophenylguanidine nitrate (**6**, R¹ = H, R² = H, R³ = NMe₂): mp 204–206 °C; RP-HPLC: t_R 9.8 min (0–60% MeCN, purity > 95%). ^{1}H NMR (DMSO-d_6): δ 2.40 (s, 3H, CH₃), 3.15 (s, 3H, CH₃), 3.16 (s, 3H, CH₃), 4.08 (bs, 1H, NH), 6.68, (d, 2H, J = 8.5 Hz, Ph-H), 6.76 (d, 1H, J = 5.5 Hz, Py-H), 7.42 (sb, 2H, NH₂), 7.54 (d, 2H, J = 8.5 Hz, Ph-H), 8.22 (d, 1H, J = 5.5 Hz, Py-H), 9.04 (sb, 1H, NH). ^{13}C NMR (DMSO-d_6): δ 14.73, 19.06, 21.40, 60.44, 106.61, 113.57, 119.04, 121.16, 131.41, 146.68, 152.22, 158.20, 159.30,

160.41, 169.40, 171.01. MS (ESI$^+$) m/z 327.12 [M + H]$^+$. Anal. (C$_{16}$H$_{18}$N$_6$S) C, H, N.

Crystallography. The CDK2 crystals were grown by vapor diffusion using the hanging drop method. Typically, a 2-μL solution of CDK2 (7−8 mg/mL in the final purification buffer) was mixed with 2 μL of precipitant solution containing 15% PEG-6000 and 100 mM NaHEPES buffer (pH 7.8 ∼ 8.2) and gave crystals of diffraction quality. Crystals were obtained after 3−5 days at 4 °C and were about 0.05 mm in length. Complexes were prepared by soaking native CDK2 crystals in a solution containing ligand. The soaking solutions used for **21**, **25**, and **32** consisted of 5 mM ligand, 20% PEG-6000, and 100 mM HEPES (pH 7.8). For **32**, the soaking solution was supplemented with 5% EtOH. Crystals were soaked for up to 2 h. For **37** crystals were transferred to a solution containing 40% PEG-4000, 0.1 M Na HEPES buffer (pH 7.4) and 15 mM NaCl from a starting solution of 20% PEG-4000. PEG-4000 concentration was increased by 5% using 30 min intervals. The final soaking solution contained 5% DMSO and 0.5 mM, and soaking was performed for 10 d. Crystals were mounted in 0.05−0.1 mm cryo-loops (Hampton Research). The crystals were immersed briefly in a cryoprotectant and then flash-frozen in liquid N$_2$. The cryoprotectant used was 100% immersion oil, except for **37**, where the soaking solution acted as the cryoprotectant.

All diffraction data (Table 2) were collected at 100 K (Cryostream, Oxford Cryosystems). Data for CDK2 complexes with **21**, **25**, and **32** were collected at the Daresbury (England) synchrotron facility on stations 14.1 or 9.6 using an ADSC Quantum4. Data processing was carried out using the programs DENZO and SCALEPACK.[35] Data for **37** were collected at the European synchrotron radiation facility (ESRF, Grenoble, France) on station 14 eh2. Data processing was carried out using the program MOSFLM.[36] The molecular replacement program MOLREP[37] using PDB entries 1HCL or 1CKP as the search model was used to solve the structures. REFMAC,[38] SHELX97,[39] and CNS[40] were used for structural refinement. Occupancy refinement of ligands was performed using the programs SHELX97. A number of rounds of refinement and model-building with the program O[41] were carried out. The coordinates of the complex structures were deposited with the Protein Data Bank under the following accession codes: 1PXM (**21**), 1PXN (**25**), 1PXO (**32**), and 1PXP (**37**).

Kinase Assays. These were carried out as described.[18] CDK 7 and 9 assays: peptide substrate (biotinyl-Ahx-(Tyr-Ser-Pro-Thr-Ser-Pro-Ser)$_4$-NH$_2$; 1−2 mg/mL) and recombinant human CDK7/cyclin H or CDK9/cyclin T1 (0.5−2 μg) were incubated for 45 min at 30 °C in the presence of varying amounts of test compound in 20 mM MOPS pH 7.2, 25mM β-glycerophosphate, 5 mM EGTA, 1 mM DTT, 1 mM sodium vanadate, 15 mM MgCl$_2$, and 100 μM ATP (containing a trace amount of ^{32}PγATP) in a total volume of 25 μL in a 96-well microtiter plate. The reaction was stopped by placing the plate on ice for 2 min. Avidin (50 μg) was added to each well, and the plate was incubated at room temp for 30 min. The samples were transferred to a 96-well P81 filter plate and washed (4 × 200 μL per well) with 75 mM phosphoric acid. Microscint 40 scintillation liquid (50 μL) was added to each well, and the amount of ^{32}P incorporation for each sample was measured using a Packard Topcount microplate scintillation counter. IC$_{50}$ values were calculated from dose−response curves (GraphPad Prism curve-fitting software); from these calculated apparent inhibition constants (K_i) were obtained using the Cheng−Prusoff[42] equation: $K_i = \text{IC}_{50}/(1 + ([\text{ATP}]/K_{\text{m (app) ATP}}))$, where [ATP] is the ATP concentration used for the IC$_{50}$ determination and $K_{\text{m (app) ATP}}$ for each kinase was determined experimentally.

Cytotoxicity Assays. Standard MTT (thiazolyl blue; 3-[4,5-dimethylthiazol-2-yl]-2,5-diphenyltetrazolium bromide) assays were performed.[43] In short, cells were seeded into 96-well plates according to doubling time and incubated overnight at 37 °C. Test compounds were made up in DMSO, and a 3-fold dilution series prepared in 100 μL of cell medium, added to cells (in triplicates), and incubated for 72 or 96 h at 37 °C. MTT was made up as a stock of 5 mg/mL in cell medium, and

the solution was filter-sterilized. Medium was removed from cells followed by a wash with 200 μL/well PBS. MTT solution was then added at 20 μL/well and incubated in the dark at 37 °C for 4 h. MTT solution was removed and cells were again washed with 200 μL of PBS. MTT dye was solubilized with 200 μL/well of DMSO with agitation. Absorbance was read at 540 nm and data analyzed using curve-fitting software (Graph-Pad Prism) to determine IC$_{50}$ values. The cell lines used were obtained from the ATCC (American Type Culture Collection, Manessas, VA).

Immunoblotting. A549 Human lung carcinoma epithelial cells were seeded at 2 × 10^5 cells/well of a six-well plate (9.6 cm^2 growth area) in DMEM media (Sigma) supplemented with FCS and P/S. Compound **32** (in DMSO) was added 24 h later, and cells were harvested at the appropriate time point by removing media and scraping with 0.7 mL of harvesting buffer. Harvesting buffer consisted of ice cold PBS, 0.1% protease inhibitor cocktail (Sigma), 100 mM NaF, and 1 mM Na$_3$VO$_4$. Cells were spun at 10 000g for 10 min at 4 °C. Cell culture lysis reagent (5 ×; Promega), diluted with harvesting buffer, was added to cell pellets, and the mixtures were snap frozen in liquid N$_2$. Cell lysates were normalized using a protein estimation protocol (Bio-Rad). Lysate (15 μg) was electrophoresed on NuPAGE 10% Bis-Tris gels. Proteins were transferred to a nitrocellulose membrane for immunoprobing. The membrane was probed using antibodies against total pRb (IF-8, clone produced in-house), pRb pT821, pRb pS249/T252 (Biosource), RNAP II Ser-2 (Covance), and RNAP II Ser-5 (Europa). Detection was achieved using ECL-plus (Amersham). Blots were stripped using the recommended protocol (100 mM 2-mercaptoethanol, 2% SDS, 62.5 mM Tris-HCl pH 6.7 at 50 °C for 30 min) and reprobed.

Synchronization of Cells at G1/S and Cell Cycle Analysis by FACS. A549 cells were synchronized at the G1/S boundary by sequentially blocking in thymidine, followed by mimosine. The cells were plated at 5 × 10^5 cells on 10 cm^2 dishes and grown at 37 °C for 24 h. Thymidine (2 mM) was added to the medium, and the cells were incubated at 37 °C for 18 h. The cells were released from thymidine block by removing the medium, washing three times in PBS, and then adding fresh medium. Cells were incubated for 6 h before adding 0.5 mM mimosine. After a further 16 h incubation, the cells were released from mimosine block as described above, and fresh medium was added containing 0.5 μM compound **32**. Cells were fixed for FACS analysis at several time points after release from block. Cells were trypsinized to release them from the plate and were fixed for 10 min at 37 °C in 1% formaldehyde in PBS. They were washed once in PBS, fixed in 70% ethanol, and stored at −20 °C for at least 24 h.

For FACS analysis, cells were pelleted, washed twice in PBS/1% BSA, and incubated in PBS, 1% BSA, and 0.25% Triton X-100 on ice for 15 min. Cells were pelleted and incubated with FITC-conjugated cyclin B1 antibody (Pharmingen 554108) diluted 1:10 for 1 h at room temperature. Cells were washed twice in 1 mL PBS/1% BSA and incubated in PBS containing 36 μg/mL RNAse A and 125 μg/mL propidium iodide for 30 min at 37 °C. Analysis of DNA content measured by propidium iodide fluorescence (FL3 channel) and cyclin B levels measured by FITC fluorescence (FL1 channel) was performed on a BD-FACSCalibur flow cytometer (Becton Dickinson).

Immunostaining. HeLa cells grown on coverslips and treated with compound **32** were fixed in cold methanol (−20 °C) for 3 min, dried, and stored at −80 °C. The coverslips were washed three times with PBT (PBS, 0.1% Triton X-100) and once with PBS and then incubated for 2 h at room temperature with primary antibodies: (rat anti-α-tubulin (YL1/2 Serotec MCAP77) diluted 1:500, rabbit anti-γ-tubulin (Sigma DQ-19) diluted 1:1000 in PBS/1% BSA. They were then washed three times with PBT and incubated for 1 h at room temperature with secondary antibodies (TRITC-conjugated donkey anti-rat IgG (Jackson 712−026−150) and Alexafluor Green 488-conjugated goat anti-rabbit IgG (Molecular Probes A11008) diluted 1:300. Cells were washed as described above,

incubated for 2 min in PBS containing 0.5 μg/mL DAPI, and mounted in *n*-propyl gallate medium. An assessment of percentages of mitotic cells, multinuclear cells, and dead cells (with highly fragmented and condensed nuclear material) was made after counting >1000 cells on each slide.

References

(1) Malumbres, M.; Barbacid, M. To cycle or not to cycle: a critical decision in cancer. *Nat. Rev. Cancer* **2001**, *1*, 222−231.
(2) Kitagawa, M.; Higashi, H.; Suzuki-Takahashi, I.; Segawa, K.; Hanks, S. K.; et al. Phosphorylation of E2F-1 by cyclin A-cdk2. *Oncogene* **1995**, *10*, 229−236.
(3) Krek, W.; Xu, G.; Livingston, D. M. Cyclin A-kinase regulation of E2F-1 DNA binding function underlies suppression of an S phase checkpoint. *Cell* **1995**, *83*, 1149−1158.
(4) Chen, Y.-N. P.; Sharma, S. K.; Ramsey, T. M.; Jiang, L.; Martin, M. S.; et al. Selective killing of transformed cells by cyclin/cyclin-dependent kinase 2 antagonists. *Proc. Natl. Acad. Sci. U.S.A.* **1999**, *96*, 4325−4329.
(5) Napolitano, G.; Majello, B.; Lania, L. Role of cyclinT/Cdk9 complex in basal and regulated transcription (Review). *Int. J. Oncol.* **2002**, *21*, 171−177.
(6) Fischer, P. M.; Endicott, J.; Meijer, L. Cyclin-dependent kinase inhibitors. *Progress in Cell Cycle Research*; Editions de la Station Biologique de Roscoff: Roscoff, France, 2003; pp 235−248.
(7) Hardcastle, I. R.; Golding, B. T.; Griffin, R. J. Designing inhibitors of cyclin-dependent kinases. *Annu. Rev. Pharmacol. Toxicol.* **2002**, *42*, 325−348.
(8) Toogood, P. L. Cyclin-dependent kinase inhibitors for treating cancer. *Med. Res. Rev.* **2001**, *21*, 487−498.
(9) Fischer, P. M.; Gianella-Borradori, A. CDK inhibitors in clinical development for the treatment of cancer. *Exp. Opin. Invest. Drugs* **2003**, *12*, 955−970.
(10) Sausville, E. A. Complexities in the development of cyclin-dependent kinase inhibitor drugs. *Trends Mol. Med.* **2002**, *8*, S32−S37.
(11) van den Heuvel, S.; Harlow, E. Distinct roles for cyclin-dependent kinases in cell cycle control. *Science* **1993**, *262*, 2050−2054.
(12) Hu, B.; Mitra, J.; Van den Heuvel, S.; Enders, G. H. S and G2 phase roles for Cdk2 revealed by inducible expression of a dominant-negative mutant in human cells. *Mol. Cell. Biol.* **2001**, *21*, 2755−2766.
(13) Tetsu, O.; McCormick, F. Proliferation of cancer cells despite CDK2 inhibition. *Cancer Cell* **2003**, *3*, 233−245.
(14) Ortega, S.; Prieto, I.; Odajima, J.; Martin, A.; Dubus, P.; et al. Cyclin-dependent kinase 2 is essential for meiosis but not for mitotic cell division in mice. *Nat. Genet.* **2003**, *35*, 25−31.
(15) Berthet, C.; Aleem, E.; Coppola, V.; Tessarollo, L.; Kaldis, P. Cdk2 knockout mice are viable. *Curr. Biol.* **2003**, *13*, 1775−1785.
(16) McClue, S. J.; Blake, D.; Clarke, R.; Cowan, A.; Cummings, L.; et al. In vitro and in vivo antitumor properties of the cyclin dependent kinase inhibitor CYC202 (R-roscovitine). *Int. J. Cancer* **2002**, *102*, 463−468.
(17) Lees, J. A.; Weinberg, R. A. Tossing monkey wrenches into the clock: new ways of treating cancer. *Proc. Natl. Acad. Sci. U.S.A.* **1999**, *96*, 4221−4223.
(18) Wu, S. Y.; McNae, I.; Kontopidis, G.; McClue, S. J.; McInnes, C.; et al. Discovery of a Novel Family of CDK Inhibitors with the Program LIDAEUS: Structural Basis for Ligand-Induced Disordering of the Activation Loop. *Structure* **2003**, *11*, 399−410.
(19) Bredereck, H.; Effenberger, F.; Botsch, H. Acid amide reactions. XLV. Reactivity of formamidines, dimethylformamide diethyl acetal (amide acetal), and bis(dimethylamino)methoxymethane (aminal ester). *Chem. Ber.* **1964**, *97*, 3397−3406.
(20) Zimmermann, J.; Caravatti, G.; Mett, H.; Meyer, T.; Müller, M.; et al. Phenylamino-pyrimidine (PAP) derivatives: a new class of potent and selective inhibitors of protein kinase C (PKC). *Arch. Pharm. Pharm. Med. Chem.* **1996**, *329*, 371−376.

(21) Schulze-Gahmen, U.; De Bondt, H. L.; Kim, S. H. High-resolution crystal structures of human cyclin-dependent kinase 2 with and without ATP: bound waters and natural ligand as guides for inhibitor design. *J. Med. Chem.* **1996**, *39*, 4540−4546.
(22) Russo, A. A.; Jeffrey, P. D.; Pavletich, N. P. Structural basis of cyclin-dependent kinase activation by phosphorylation. *Nat. Struct. Biol.* **1996**, *3*, 696−700.
(23) Knockaert, M.; Greengard, P.; Meijer, L. Pharmacological inhibitors of cyclin-dependent kinases. *Trends Pharmacol. Sci.* **2002**, *23*, 417−425.
(24) Zarkowska, T.; Mittnacht, S. Differential phosphorylation of the retinoblastoma protein by G1/S cyclin-dependent kinases. *J. Biol. Chem.* **1997**, *272*, 12738−12746.
(25) Oelgeschlager, T. Regulation of RNA polymerase II activity by CTD phosphorylation and cell cycle control. *J. Cell. Physiol.* **2002**, *190*, 160−169.
(26) Hughes, T. A.; Cook, P. R. Mimosine arrests the cell cycle after cells enter S-phase. *Exp. Cell Res.* **1996**, *222*, 275−280.
(27) Jackson, P. K.; Chevalier, S.; Philippe, M.; Kirschner, M. W. Early events in DNA replication require cyclin E and are blocked by p21CIP1. *J. Cell. Biol.* **1995**, *130*, 755−769.
(28) Ohtsubo, M.; Theodoras, A. M.; Schumacher, J.; Roberts, J. M.; Pagano, M. Human cyclin E, a nuclear protein essential for the G1-to-S phase transition. *Mol. Cell. Biol.* **1995**, *15*, 2612−2624.
(29) Strausfeld, U. P.; Howell, M.; Descombes, P.; Chevalier, S.; Rempel, R. E. et al. Both cyclin A and cyclin E have S-phase promoting (SPF) activity in Xenopus egg extracts. *J. Cell Sci.* **1996**, *109*, 1555−1563.
(30) Coverley, D.; Laman, H.; Laskey Ronald, A. Distinct roles for cyclins E and A during DNA replication complex assembly and activation. *Nat. Cell Biol.* **2002**, *4*, 523−528.
(31) Pagano, M.; Pepperkok, R.; Verde, F.; Ansorge, W.; Draetta, G. Cyclin A is required at two points in the human cell cycle. *EMBO J.* **1992**, *11*, 961−971.
(32) Lukas, C.; Sorensen, C. S.; Kramer, E.; Santoni-Ruglu, E.; Lindeneg, C.; et al. Accumulation of cyclin B1 requires E2F and cyclin-A-dependent rearrangement of the anaphase-promoting complex. *Nature* **1999**, *401*, 815−818.
(33) Ljungman, M.; Paulsen, M. T. The cyclin-dependent kinase inhibitor roscovitine inhibits RNA synthesis and triggers nuclear accumulation of p53 that is unmodified at Ser15 and Lys382. *Mol. Pharmacol.* **2001**, *60*, 785−789.
(34) Chao, S.-H.; Price, D. H. Flavopiridol inactivates P-TEFb and blocks most RNA polymerase II transcription in vivo. *J. Biol. Chem.* **2001**, *276*, 31793−31799.
(35) Otwinowski, Z.; Minor, W. Processing of X-ray diffraction data collected in oscillation mode. *Methods Enzymol.* **1997**, *276*, 307−326.
(36) Leslie, A. G. W. Recent changes to the MOSFLM package for processing film and image plate data. *Joint CCP4 + ESF-EAMCB Newsletter on Protein Crystallography*; 1992, No. 26. http://www.ccp4.ac.uk/main.html.
(37) Vagin, A.; Teplyakov, A. MOLREP: an automated program for molecular replacement. *J. Appl. Crystallogr.* **1997**, *30*, 1022−1025.
(38) Murshudov, G. N.; Vagin, A. A.; Dodson, E. J. Refinement of macromolecular structures by the maximum-likelihood method. *Acta Crystallogr.* **1997**, *D53*, 240−255.
(39) Sheldrick, G. M.; Schneider, T. R. SHELXL: high-resolution refinement. *Methods Enzymol.* **1997**, *277*, 319−343.
(40) Brunger, A. T.; Adams, P. D.; Clore, G. M.; DeLano, W. L.; Gros, P.; et al. Crystallography & NMR System: a new software suite for macromolecular structure determination. *Acta Crystallogr.* **1998**, *D54*, 905−921.
(41) Jones, T. A.; Zou, J. Y.; Cowan, S. W.; Kjeldgaard, M. Improved methods for building protein models in electron density maps and the location of errors in these models. *Acta Crystallogr., Sect. A: Found. Crystallogr.* **1991**, *A47*, 110−119.
(42) Cheng, Y. C.; Prusoff, W. H. Relationship between the inhibition constant (K_i) and the concentration of inhibitor which causes 50% inhibition (IC$_{50}$) of an enzymatic reaction. *Biochem. Pharmacol.* **1973**, *22*, 3099−3108.
(43) Haselsberger, K.; Peterson, D. C.; Thomas, D. G.; Darling, J. L. Assay of anticancer drugs in tissue culture: comparison of a tetrazolium-based assay and a protein binding dye assay in short-term cultures derived from human malignant glioma. *Anti Cancer Drugs* **1996**, *7*, 331−338.